JVI Journals.ASM.org

Early Function of the Abutilon Mosaic Virus AC2 Gene as a Replication Brake

Björn Krenz,* Kathrin Deuschle, Tobias Deigner, Sigrid Unseld, Gabi Kepp, Christina Wege, Tatjana Kleinow, Holger Jeske

Institut für Biomaterialien und Biomolekulare Systeme, Abteilung für Molekularbiologie und Virologie der Pflanzen, Universität Stuttgart, Stuttgart, Germany

ABSTRACT

The C2/AC2 genes of monopartite/bipartite geminiviruses of the genera *Begomovirus* and *Curtovirus* encode important pathogenicity factors with multiple functions described so far. A novel function of *Abutilon* mosaic virus (AbMV) AC2 as a replication brake is described, utilizing transgenic plants with dimeric inserts of DNA B or with a reporter construct to express green fluorescent protein (GFP). Their replicational release upon AbMV superinfection or the individual and combined expression of epitope-tagged AbMV AC1, AC2, and AC3 was studied. In addition, the effects were compared in the presence and in the absence of an unrelated tombusvirus suppressor of silencing (P19). The results show that AC2 suppresses replication reproducibly in all assays and that AC3 counteracts this effect. Examination of the topoisomer distribution of supercoiled DNA, which indicates changes in the viral minichromosome structure, did not support any influence of AC2 on transcriptional gene silencing and DNA methylation. The geminiviral AC2 protein has been detected here for the first time in plants. The experiments revealed an extremely low level of AC2, which was slightly increased if constructs with an intron and a hemagglutinin (HA) tag in addition to P19 expression were used. AbMV AC2 properties are discussed with reference to those of other geminiviruses with respect to charge, modification, and size in order to delimit possible reasons for the different behaviors.

IMPORTANCE

The (A)C2 genes encode a key pathogenicity factor of begomoviruses and curtoviruses in the plant virus family *Geminiviridae*. This factor has been implicated in the resistance breaking observed in agricultural cotton production. AC2 is a multifunctional protein involved in transcriptional control, gene silencing, and regulation of basal biosynthesis. Here, a new function of *Abutilon* mosaic virus AC2 in replication control is added as a feature of this protein in viral multiplication, providing a novel finding on geminiviral molecular biology.

Viral proteins may have multiple functions, even if they are small, such as the (A)C2 gene products (~14 kDa and ~130 amino acids [aa]) of geminiviruses. Over the past decades, several functions have been elucidated for different geminiviruses by using different experimental assays, but how all of them work together in the context of viral infection and symptom development is still an enigma.

The family *Geminiviridae* now comprises seven genera (1), with members harboring one (monopartite; DNA A-like) or two (bipartite; DNA A and DNA B) circular DNA components. They are classified according to their host plants (monocot or dicot) and insect vectors (whitefly or leafhopper). Viruses of the genera *Begomovirus* and *Curtovirus* have mostly been investigated to characterize the function of the open reading frame (ORF) (A)C2 [syn., (A)L2], a name originally coined due to its expression from the complementary (leftward) strand and the second transcript of DNA A or the DNA A-like monopartite genome components (Fig. 1a). Mastreviruses lack a homolog of AC2 (2). Consequently, this gene is not fundamentally necessary for the geminiviral life cycle and rather may add some evolutionary advantage in the epidemic race between geminivirus and dicot host plant defense.

The current knowledge about this gene is based on diverse experimental approaches, such as ectopic expression from plasmids in plant protoplasts, bacteria, or yeast cells; one- or two-hybrid screens in yeast; promoter studies in single cells or tissues and plants; and transcriptomic and metabolic studies in plants, leading to a large amount of literature, which cannot be cited here completely due the lack of space.

Analyses of different geminiviruses with different techniques have revealed many aspects of (A)C2 functions, and a puzzling, complex mosaic picture has arisen (for recent reviews, see references 2–5). Originally, a second name, "transcriptional activator protein" (TrAP), was coined for the AC2 gene product of the New World begomovirus tomato golden mosaic virus (TGMV), since it can activate the expression of the viral sense genes AV1 and BV1 for coat protein (CP) and nuclear shuttle protein (NSP), respectively (6–11). However, the TGMV AC2 protein does not bind directly to geminiviral promoters but influences the expression of viral proteins indirectly and in a complex manner, as shown by whole-plant assays (11–15). Although similar in other aspects, as discussed below, the homologous C2 gene of curtoviruses at the

Received 4 December 2014 **Accepted** 10 January 2015

Accepted manuscript posted online 14 January 2015

Citation Krenz B, Deuschle K, Deigner T, Unseld S, Kepp G, Wege C, Kleinow T, Jeske H. 2015. Early function of the abutilon mosaic virus AC2 gene as a replication brake. J Virol 89:3683–3699. doi:10.1128/JVI.03491-14.

Editor: A. Simon

Address correspondence to Holger Jeske, holger.jeske@bio.uni-stuttgart.de.

* Present address: Björn Krenz, Lehrstuhl für Biochemie, Department Biologie, Erlangen, Germany.

B.K. and K.D. contributed equally to this work.

doi:10.1128/JVI.03491-14

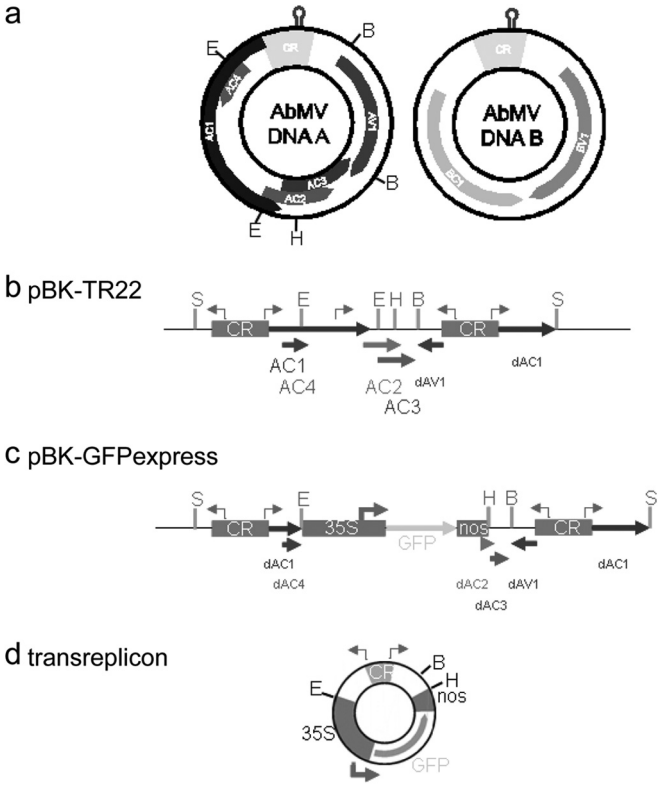

FIG 1 Genome maps of constructs used in this study. (a) wt *Abutilon* mosaic virus DNA components DNA A and DNA B. (b) Linear version of a DNA A derivative (pBK-TR22) lacking the coat protein gene (dAV1), with two common regions (CR); the intact ORFs for AC1 (replication initiator protein Rep), AC4, AC2 (transcription activator protein [TrAP]), and AC3 (replication enhancer [REn]), the direction of bidirectional transcription (kinked arrows); and the used restriction enzyme recognition sites for SalI (S), EcoRI (E), HindIII (H), and BamHI (B), as described previously (56). (c) Construct derived from pBK-TR22 with an insertion of the 35S promoter (35S), the green fluorescent protein (GFP) gene, and the nos terminator between the EcoRI and HindIII sites replacing or inactivating all geminiviral coding sequences (dACx and dAVx). (d) Transreplicon as expected from the replicational release of the GFPexpress construct upon AbMV superinfection.

same genome position has not been found to transactivate viral genes (16).

On the molecular level, TGMV AC2 binds single-stranded DNA (ssDNA), possesses a zinc finger and a transactivation domain, and is regulated by phosphorylation (17). Phosphorylation of AC2 proteins from cabbage leaf curl virus (CaLCuV) and tomato mottle virus (ToMoV), both New World begomoviruses, was recently shown to be important for infection (18). C2 of tomato yellow leaf curl virus-China (TYLCV-C) (19) was localized to nuclei, whereas TGMV AC2 was found in nuclei and the cytoplasm (20), by using different techniques and cells.

(A)C2 proteins have been found to interact with proteins of the basal cell metabolism, including adenosine kinase and SNF1 kinase, and influence the methyl cycle (20–25). Correspondingly, a large set of transcripts are differentially expressed upon (A)C2 production in transient assays and transgenic plants (26–31), with some harmful effects (32).

Abutilon mosaic virus (AbMV) is a bipartite begomovirus originally from the New World (West Indies islands), with a special history, as it has been propagated intentionally in ornamental plants worldwide by gardeners (33, 34). During 150 years of vegetative propagation of infected host plants, the virus has been attenuated and has lost its capability of whitefly transmission (35). Although it is still able to induce severe symptoms in test plants such as *Malva parviflora*, only mild symptoms are observed in the model plant *Nicotiana benthamiana* (33, 36, 37). Since AC2 is a major pathogenicity determinant for geminiviruses, this history of AbMV may have also modulated the AC2 function, but no gross changes in the protein sequence can be observed when AbMV AC2 is compared with TGMV AC2, a closely related begomovirus (38) that has been investigated in great detail in this respect. AbMV AC2 is able to activate transcription in one-hybrid yeast assays (A. Aberle and H. Jeske, unpublished data) and is necessary for systemic infection (39) but is not essential for any of the three modes of viral replication (40): complementary-strand replication (CSR), rolling-circle replication (RCR), and recombination-dependent replication (RDR).

Geminiviruses build minichromosomes as intermediates for transcription and replication (41–44), which may be targets of DNA and histone methylation (3, 45). Since AC2 has been shown to influence the cellular methyl cycle, it was interesting to investigate whether its overexpression can change the minichromosome architecture by DNA methylation. Since nucleosome loading is reflected by the number of superhelical turns per covalently closed circular DNA (cccDNA) molecule (42), the coverage (condensation degree) of minichromosomes can be monitored by determining the topoisomer distribution of cccDNA (46). Moreover, the use of methylation-dependent restriction enzymes (e.g., McrBC) allows the detection of methylation on these specific DNA forms, a prerequisite for the evaluation of geminiviral DNA in this context (41). A regular shift from topoisomers indicating a loading with 12 to 13 nucleosomes was observed previously for AbMV-infected aging leaves of ornamental *Abutilon* plants under steady-state infection conditions (41, 42). Since 13 nucleosomes cover the geminiviral 2,632-nucleotide (nt)-long cccDNA completely, whereas 12 nucleosomes leave a gap for the assembly of transcription factors (42), the topoisomer distribution may indicate transcriptionally inactive and active viral genomes, respectively. During the course of systemic infection of *N. benthamiana* plants, however, young leaf samples revealed only sporadic minichromosomes with 13 nucleosomes at maximum (46).

Starting with questions about transcription control in combination with gene silencing, the following experiments instead revealed a surprising novel role of AbMV AC2: the protein appears to slow down replication, acting as a replication brake.

MATERIALS AND METHODS

Microorganisms, plants, and general methods. Agroinfectious clones of AbMV DNA A and DNA B (47) (GenBank accession no. NC_001928 and NC_001929) were used for infection and as a source for further constructs. An agrobacterial expression clone for the *Cymbidium* ringspot virus (CymRSV) silencing suppressor (P19) was kindly provided by D. Silhavy (48). All binary vectors used in this study (pPCV812-Menchu-Rep, pPCV812-Menchu-TrAP, pPCV002-Gigi-REn, and pBIN-GFP-express) were introduced into chemically competent *Agrobacterium tumefaciens* strain GV3101(pMP90) (49). The correctness of the inserts was confirmed by PCR and sequencing. *N. benthamiana* Domin plants were grown in an insect-free S2 greenhouse with 16 h of supplementary illumination, as described previously (37). *Escherichia coli* protein expression constructs were described previously (50).

Cloning of viral constructs. Recombinant DNA techniques were performed according to methods described previously (51). Restriction endonucleases and DNA-modifying enzymes were used as recommended by the manufacturers. DNA sequencing confirmed the correctness of the respective constructs. Sequence alignment was done by using Vector NTI (Invitrogen, Life Technologies, Darmstadt, Germany).

For the expression of hemagglutinin (HA)-tagged AbMV AC2 *in planta*, the coding region of the AC2 gene was amplified by PCR (30 cycles of 30 s at 90°C, 30 s at 58°C, and 1 min at 72°C, followed by 5 min at 72°C), using an AbMV DNA A clone (47) as the template and the primer pair 5′-AGGATCCTAATGCGATCTTCATCACCCTCA-3′ and 5′-AGGATCCGTCGACCTATTTAAATAAATTGACCCAGAA-3′ (added BamHI cleavage sites are underlined). The PCR product was inserted by TA cloning into pGEM-T (Promega, Mannheim, Germany). The resulting insert was transferred into the binary vector pPCV812-Menchu (52), using the BamHI restriction sites for exchange, yielding a fusion of the AC2 ORF with an intron-disrupted coding sequence for the HA epitope present in the vector. The expression construct for c-myc-tagged AbMV AC3 was generated similarly by PCR amplification of the AC3 ORF (primer pair 5′-AGGATCCTAATGGATTCACGCACAGGGGAA T-3′ and 5′-AGGATCCGTCGACTTAATAAAATTTGAATTTTATTGA-3′), cloning into pGEM-T, and insertion of the verified AC3 fragment into the binary vector pPCV002-Gigi (52). This construct expresses AC3 in fusion with an intron-disrupted coding sequence of the c-myc epitope. Cloning of the expression construct for HA-tagged AbMV Rep (pPCV812-Menchu-Rep) was described previously (53). Transgenic plants carrying dimers of AbMV DNA B ("DNA-B plants") were stable T4 progenies of those described previously (54).

For the control, a mutant AC2 construct was established by cleaving pPCV812-Menchu-TrAP with BamHI under limiting conditions to cleave only one site, followed by a fill-in reaction with Klenow enzyme and religation. After transformation into bacteria, the correct construct was identified by sequencing and used for agroinfiltration. This manipulation results in a frameshift (fs), which still retains the expression of the HA tag but now fuses the last amino acids of AC1 instead of AC2 (named HA:AC2fs). Except for the nucleotides added during the fill-in reaction, the expected transcript was not altered in comparison with the HA:AC2 construct.

Transreplicon cloning. To generate pBK-GFPexpress, the mutated green fluorescent protein 4 (mGFP4) expression cassette containing a cauliflower mosaic virus (CaMV) 35S promoter and a nopalin synthase (nos) terminator (55) was transferred into pBK-TR22 (56) by insert exchange between the restriction sites EcoRI and HindIII (Fig. 1b). The recombinant cassette was released by SalI digestion and inserted into SalI-linearized pBINplus (57), resulting in pBIN-GFPexpress.

Plant transformation and inoculation. Transgenic *N. benthamiana* plants were generated by transforming leaf discs using *A. tumefaciens* GV3101(pMP90) carrying the binary plasmid pBIN-GFPexpress using antibiotic selection (100 μg of kanamycin/ml and Murashige-Skoog basal salts medium no. 5524 supplemented with vitamins and phytohormones; Sigma, Munich, Germany). Shoots from transgenic callus were placed on root and selection medium (without 6-benzylaminopurine and indole-3-acetic acid) to regenerate whole transgenic plants in a controlled-environment light chamber at 22°C to 24°C with a 16-h photoperiod. Transformed plantlets were identified by PCR using mGFP4-specific primers (56).

Agroinfiltration assay. Plasmid-containing agrobacteria were grown overnight, pelleted, resuspended in 10 mM $MgCl_2$ and 100 μM acetosyringone, diluted to an optical density at 600 nm (OD_{600}) of 0.5, and incubated for at least 2 h at room temperature. Source leaves of 5- to 6-week-old *N. benthamiana* plants were injured with a needle, and the respective agrobacterial suspensions were infiltrated with a 5-ml syringe according to methods described previously (58).

Virus detection. Rolling-circle amplification combined with restriction fragment length polymorphism (RCA/RFLP) analysis was used to detect viral DNA from inoculated plants. Using total nucleic acids (10 ng) from systemically infected plant tissues as the template and a TempliPhi DNA amplification kit (GE Healthcare, Freiburg, Germany), DNA was synthesized at 30°C for at least 16 h according to methods described previously (59). The reaction was stopped at 65°C for 10 min, and the RCA products were digested with EcoRI.

Analysis of viral DNA conformations. Total nucleic acids from plant tissues were prepared, using extraction buffer (100 mM Tris-HCl [pH 7.0], 100 mM NaCl, 10 mM EDTA, 1% sodium dodecyl sulfate [SDS], 10 mM *N*-ethylmaleimide [NEM], 100 mM dithiothreitol [DTT]), and phenol-chloroform (twice; 1:1) and chloroform extraction and ethanol precipitation (once) (41). Three hundred nanograms of total DNA per sample was separated by electrophoresis on 1.4% agarose gels supplemented with 10 μg/ml chloroquine in the gel as well as in the Tris-boric acid-EDTA (TBE) buffer tank and transferred onto Hybond N+ membranes (GE Healthcare). Viral DNAs were detected by digoxigenin-labeled probes, according to the manufacturer's recommendations (DIG-High Prime kit; Roche, Mannheim, Germany), and by chemiluminescence, as previously described (40).

Small interfering RNA detection. For small interfering RNA (siRNA) detection, total RNA was extracted from 100 mg plant tissue by using TRIzol reagent (Invitrogen, Darmstadt, Germany), according to the manufacturer's protocol, and dissolved in 15 μl loading buffer (95% formamide, 20 mM EDTA [pH 8.0], 0.05% bromophenol blue, and 0.05% xylene cyanol), heated at 70°C for 5 min, and separated on 12% polyacrylamide (PA) minigel (8.3 by 7.3 cm; acrylamide-bisacrylamide [19:1], 7 M urea) at 70 V for 4 h. RNA was transferred onto a Hybond NX membrane by electroblotting in 0.5× TBE buffer for 1 h (semidry blotting apparatus; Bio-Rad, Munich, Germany). Hybridization was performed according to methods described previously (60), using digoxigenin-labeled RNAs (DIG-RNA labeling kit; Roche) as the probe. The blot was washed twice with 2× SSC (1× SSC is 0.15 M NaCl plus 0.015 M sodium citrate)–0.5% SDS for 30 min at 58°C. Chemiluminescence was detected with the substrate disodium 3-(4-methoxyspiro[1,2-dioxethane-3,2′-(5′-chloro) tricyclo[3.3.1.1^{3,7}]decan]-4-yl)phenylphosphate (CSPD), according to the manufacturer's protocols (DIG application manual for filter hybridization; Roche).

Nonequilibrium pH gradient electrophoresis. AbMV AC2 proteins were extracted from induced *E. coli* cells with pET3a-based AC2 expression plasmids (50). Bacterial cultures (15 ml) were harvested by centrifugation (5 min at 4,000 rpm in a Heraeus Sepatech Variofuge 3.0 at 4°C), and cells were washed with 8 ml buffer (50 mM Tris-HCl [pH 8.0], 100 mM NaCl) and resuspended in 1 ml of this buffer. After the addition of 6 ml of a phenol solution (50% in 0.1 M Tris-HCl [pH 8.0], 5% 2-mercapthoethanol), the suspension was shaken for 30 min at 4°C, and phase separation was achieved by centrifugation (15 min at 4,000 rpm in a Variofuge at 4°C). The phenol phase was collected and washed with an equal volume of phenol-saturated buffer (0.1 M Tris-HCl [pH 8.0], 5% 2-mercaptoethanol). The proteins in the phenol phase were precipitated by the addition of 4 volumes of a methanolic solution of 0.1 ammonium acetate at −20°C overnight. After centrifugation (10 min at 4,000 rpm in a Variofuge at 4°C), the pellet was washed six times with 5 ml each of the methanolic solution, dried under a vacuum, and stored at −70°C. For one-dimensional (1D) SDS-polyacrylamide gel electrophoresis (PAGE), the proteins were dissolved in loading buffer (50 mM Tris-HCl [pH 6.8], 100 mM dithiothreitol, 2% SDS, 0.1% bromophenol blue, 10% glycerin), heated for 5 min at 95°C, and centrifuged briefly (Eppendorf). Electrophoresis was performed in discontinuous gels with 4% and 15% PA (61), with a 30-mA current per gel at 20°C until bromophenol blue reached the end. For two-dimensional (2D) gel electrophoresis, first-dimension isoelectric nonequilibrium pH gradient electrophoresis (NEPHGE), as described previously (62), was combined with SDS-PAGE, as described above, as a second dimension. The bacterial protein pellets were dissolved in 250 μl loading buffer A (9.5 M urea, 0.5% SDS, 5% 2-mercaptoethanol, 0.2% first-dimension ampholytes [pH 3 to 10]; Serva, Heidelberg, Ger-

many) for 10 min under agitation, followed by the addition of 250 μl loading buffer B (9.5 M urea, 4% Nonidet P-40 [NP-40] nonionic detergent, 5% 2-mercaptoethanol, 4% ampholytes [pH 3 to 10]; Serva). In this protocol, SDS is used for solubilizing the proteins, and NP-40 displaces SDS afterwards.

In the first dimension, samples migrated from anode to cathode in tubes with 4% PA, 9.2 M urea, 2% NP-40, and a 5% ampholyte mixture (1.2% at pH 9 to 11, 1.6% at pH 3 to 10 [Serva], and 1.2% at pH 8 to 10.5 [Pharmacia, Uppsala, Sweden]) for 1,670 Vh. The resulting gels were silver stained according to methods described previously (63). Molecular weights and isoelectric points (pIs) were determined with reference to the marker proteins RNase A (molecular weight, 12.4; pI 10.65), myoglobin (molecular weight, 17.8; pI 7.35 and 6.9), carbonic anhydrase (molecular weight, 29; pI 6.0), and beta-lactoglobulin (molecular weights, 18.4 and 36.5; pI 5.3 and 5.15) (Serva), using Microsoft Excel spreadsheet calculations.

Western blot analysis. Protein was isolated by using TRIzol reagent (Invitrogen), according to the manufacturer's protocol, and resuspended in SDS-PAGE loading buffer (2% SDS, 10% glycerol, 0.1 M DTT, 62.5 mM Tris-HCl [pH 6.8], 0.01% bromophenol blue). The solution was boiled for 5 min and separated on 12.5% PA gels (61). Proteins were transferred onto nitrocellulose (Schleicher and Schuell, Dassel, Germany) by using a semidry transfer assembly (Bio-Rad). Green fluorescent protein (GFP) was detected by using a 1:2,500 dilution of GFP (FL):sc-8334 polyclonal antibody (Santa Cruz Biotechnology, Heidelberg, Germany), and HA-tagged fusion proteins were detected by using a 1:500 dilution of HA.11 monoclonal antibody (Covance, Munich, Germany). Blots were developed by using horseradish peroxidase (HRP)-linked anti-mouse or anti-rabbit from sheep or donkey (1:10,000) as a secondary antibody (GE Healthcare). Alternatively, for the blots shown in Fig. 11, anti-HA high-affinity rat monoclonal antibody (Roche), a goat anti-rat IgG (whole-molecule) peroxidase conjugate (Sigma), or goat anti-rabbit IgG(H+L) (Rockland, Gilbertsville, PA, USA) and the Luminata Crescendo Western HRP substrate (Millipore, Darmstadt, Germany) were used.

Microscopy and GFP imaging. Plants were screened for GFP expression under an Axiophot fluorescence microscope (with G 365, FT 395, and LP 420 filters; Zeiss, Oberkochen, Germany). Macroscopic detection of GFP fluorescence was performed by using a hand-held, long-wave UV lamp (4 W), and photographs were taken with a Canon Powershot 1 camera with a yellow filter. The images were processed by using Paint Shop Pro (Jasc Software).

Scoring of viral DNA amounts. To allow a comprehensive presentation of hybridization data for several independent experiments, comparable sets of data in parallel experiments were assigned rank numbers (1 to 4) for increasing total viral DNA signals per lane. Mean values and standard deviations were calculated for each treatment, summarizing all respective experiments.

Densitometry. The film images of gel lanes after hybridization with viral probes, as indicated in the figure legends, were scanned by using SigmaScan Pro version 5.0.0 (SPSS Inc., Erkrath, Germany) to obtain pixel intensities per line and distances of migration. A reference lane without signals was determined as the background, and the values were subtracted individually from the signal-containing lanes at the same position. The individual pixel intensities were divided by the sum of the pixel intensities per lane to obtain the relative density distribution for each sample. For transformation of the x axis to R_f values, the position of open circular DNA (ocDNA) was set to zero, the position of ssDNA was set to 1, and the quotient for the gel position $[(x_n - x_0)/(x_1 - x_0)]$ was determined by using Microsoft Excel calculation spreadsheets. These transformations compensated for different migration behaviors and viral DNA amounts in individual lanes.

Preparation of rcccDNA and topoisomer standards. GFPexpress plants were agroinfiltrated with constructs expressing HA:AC1 and P19 (48), and RCA/RFLP (EcoRI) was performed to determine the presence of the GFP transreplicon. The resulting 2,890-bp linear DNA was gel purified with the Qiaquick gel extraction kit (Qiagen, Hilden, Germany). In order to obtain monomeric circles (relaxed covalently closed circular DNA [rcccDNA]), 500 ng of the fragments was religated by T4 DNA ligase (New England BioLabs [NEB], Frankfurt am Main, Germany) in a total volume of 500 μl at 16°C overnight and diluted to a final concentration of 100 pg/μl. One nanogram of this standard was used per lane.

Three hundred microliters of rcccDNA with a concentration of 1 ng/μl was digested with 3 U exonuclease V (RecBCD; NEB) for 30 min at 37°C. The reaction was stopped with 11 mM EDTA and heat inactivated for 30 min at 70°C. Exonuclease V-treated rcccDNA (75 μl per reaction) was then incubated with 2.5 U DNA gyrase (NEB) for 30 s, 1 min, 2 min, or 4 min at 37°C, and the enzyme was heat inactivated at 65°C for 20 min. Ten microliters of each sample was analyzed on a 1.4% agarose gel containing 10 μg/ml chloroquine. Transreplicon DNA was detected by Southern blot hybridization using a GFP-specific probe to determine topoisomer distributions. The topoisomer standard was prepared by mixing equal volumes of each reaction product. Twenty microliters of the mixture was analyzed on a 2D agarose gel (first dimension, 0.75% agarose and 0.3% SDS for 22 h at 10 V; second dimension, 1.4% agarose and 10 μg/ml chloroquine for 22 h at 45 V), according to methods described previously by Jeske et al. (40). Ten microliters of this mixture per lane was used as a topoisomer standard.

Methylation-dependent restriction analysis. Three hundred nanograms of DNA was digested by using McrBC (NEB) supplemented with 100 μg/ml bovine serum albumin (BSA), 1 mM GTP, and 15 U of the restriction enzyme overnight at 37°C. Undigested samples were treated in the same way but without the addition of the enzyme. The samples were separated in 1.4% agarose gels containing 10 μg/ml chloroquine (19 h at 40 V), transferred onto a Hybond N+ membrane (GE Healthcare), and detected with a GFP-specific probe.

Exonuclease V digestion. Three hundred nanograms of DNA was digested with 3 U exonuclease V (RecBCD; NEB) for 30 min at 37°C. The reaction was stopped with 11 mM EDTA and heat inactivation for 30 min at 70°C. The samples were separated on a 1.4% agarose gel containing 10 μg/ml chloroquine (19 h at 40 V), transferred onto a Hybond N+ membrane, and detected with a GFP-specific probe.

***In silico* comparison of AC2 proteins.** Using a BLAST search, the 964 next relatives of AbMV AC2 were retrieved from the Swiss-Prot database (http://www.uniprot.org/help/uniprotkb). Molecular weights and pIs were calculated with the help of ExPasy website tools (http://web.expasy.org/compute_pi/). Further data processing was done with Microsoft Excel.

RESULTS

Plants in the following experiments were always *N. benthamiana* lines, either untransformed (wild type [wt]) as well as transgenic for a dimer of AbMV DNA B (DNA B plants) or with a transreplication cassette based on the AbMV intergenic region to express green fluorescent protein (GFPexpress plants). For agroinfiltration, all sequences of geminivirus components (DNA A, HA:AC1, HA:AC2, and myc:AC3) stem from AbMV. In addition, the cauliflower mosaic virus 35S promoter and nos terminator were applied for transcriptional control to express individual proteins. The posttranscriptional gene silencing (PTGS) suppressor P19 of an unrelated RNA virus (the tombusvirus *Cymbidium* ringspot virus) was supplied from an independent plasmid construct (48), only for comparison and to enhance protein expression.

Time course of local infections of wt virus in the absence or presence of additional AC2. To obtain a first survey of early infection events at the site of inoculation, leaves were agroinfiltrated with a combination of wt DNA A and DNA B, alone or together with a plasmid to express HA:AC2, shown for a single experiment with three independent plants treated in parallel (Fig. 2). Total nucleic acids were prepared at 3, 4, 5, and 6 days postinoc-

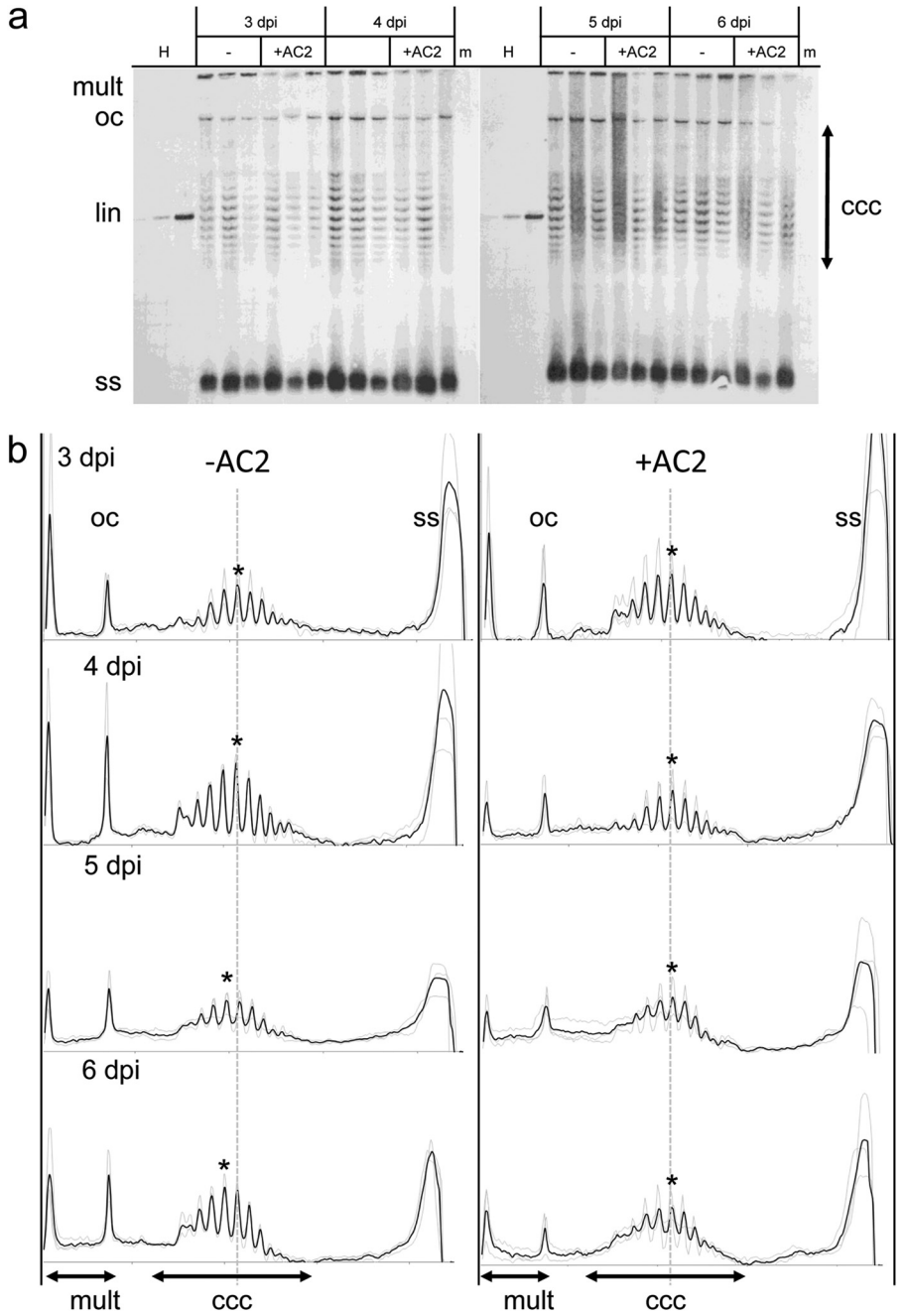

FIG 2 Local agroinfiltration of wt *N. benthamiana* leaves at 3 to 6 dpi with wt AbMV DNA A and B without (−) or with (+AC2) coinoculation of an HA:AC2-expressing plasmid. (a) Viral DNAs in total nucleic acid extracts were separated in chloroquine (10 μg/ml)-containing gels and detected by Southern blot hybridization using an AbMV DNA A probe. Three independent leaf samples are shown for each treatment. H, hybridization standard containing 1, 10, or 100 pg of linear AbMV DNA (lin); m, mock-inoculated samples. (b) Densitometric analysis of the samples shown in panel a, with pixel intensities (*y* axis) plotted against migration distance (*x* axis). In order to enable proper comparison and averaging, *y* axis values are expressed as relative intensities per lane, and *x* axis values were transformed for maximal resonance of the peaks between multimeric (mult) forms and ssDNA (ss). The resulting mean values per position are drawn as a black line, and the individual scans are shown as gray lines. Asterisks mark the most intense bands for the mean values within the flock of topoisomers of covalently closed circular DNA (ccc), with stippled dotted lines at the usually most prominent peak. oc, open circular dsDNA.

ulation (dpi) and separated on agarose gels containing chloroquine for the best resolution of the viral replication products as well as the replicative and transcriptional intermediates after blotting and hybridization (Fig. 2a). During this time course, all previously identified geminiviral DNA forms were readily detected, with some plant-to-plant variation but reproducible results. Comparison of samples with and those without overexpressed HA:AC2 revealed no significant changes in the total amount of viral DNAs that exceeded the variation between plants. This type of experiment was repeated twice, with the same results (data not shown).

The relative distribution of the DNA forms per sample as in-

ferred from scanned lanes (Fig. 2b) showed differing proportions of discrete bands and background smearing, which was more prominent in some samples at later time points. The smear indicates that more viral DNA was present in heterogeneous DNA forms after hybridization in one-dimensional (1D) gels (see, for example, the second sample at 5 dpi without AC2 and the first sample with AC2 in Fig. 2a). No differences were observed between the treatments with and those without HA:AC2 in this respect.

In spite of the different proportions of discrete bands per sample, all samples showed prominent bands for the viral cccDNA with the previously identified distribution of topoisomers (42). Only a slight shift at 5 dpi and at 6 dpi of the cccDNA maxima (Fig. 2b, asterisks) toward the left (more condensed DNA) was absent if HA:AC2 was coexpressed. Such a shift probably represents the addition of a 13th nucleosome to the open minichromosome with 12 nucleosomes, as was shown previously for AbMV DNA in older leaves of *Abutilon* plants (41, 42). However, this particular left shift at later stages of infection was not reproduced in the two subsequently repeated experiments and may be a stochastic rather than a systematic effect under these conditions (46).

In summary, early infection processes can be monitored efficiently and with highest resolution of the viral DNA forms. They yield quite reproducible results if plant-to-plant variation is carefully considered, whereas overexpression of HA:AC2 had only marginal effects in this assay.

Local agroinfiltration on DNA B plants. In the first set of experiments, AC2 was expressed from two sources, from DNA A as well as from additional expression constructs. In order to dissect the effect of AC2 on transcription and replication, individual viral genes expressed ectopically from the viral genome were compared. To achieve this, infection by wt DNA A was compared to that with various combinations of plasmids for the expression of the respective genes (AC1, AC2, and AC3), which are known to be involved in replicational or transcriptional control.

To simplify the preparation of inocula, transgenic DNA B plants were challenged. Mobilization and subsequent replication of the circular DNA B by wt DNA A or an HA:AC1-expressing plasmid were monitored by Southern blot hybridization with a DNA B-specific probe at 5 dpi (Fig. 3). In this test system, the individual effect of overexpressed HA:AC2 alone or together with myc:AC3 was examined. wt DNA A as well as singly expressed HA:AC1 were able to mobilize the DNA B transgene efficiently, although to various levels, in the 12 independent biological replicates. Surprisingly, the overexpression of HA:AC2 reduced this effect significantly. Interestingly, myc:AC3 was able to overcome the HA:AC2 effect, and replication was increased in comparison to that of the HA:AC1 samples alone. This unexpected quantitative difference was reproduced in two independent experimental sets.

Due to the plant-to-plant variation, it is not appropriate to average the individual hybridization signals. Therefore, a rank number-based evaluation was chosen to examine the reliability of the estimate for the relation of the viral titers (Table 1). With this aim, another series of low-resolution agarose gels with ethidium bromide to control the loading of total DNA were analyzed by Southern blotting hybridization. The results for parallel treatments per experiment were ranked for arbitrarily chosen plant samples in four independent experimental sets. Viral DNAs were monitored in the inoculated leaves and, in addition, in potentially systemically infected new emerging leaves. The presence of viral DNA A and DNA B was further scrutinized by the extremely sensitive RCA/RFLP method, followed by hybridization with DNA A or DNA B probes, in order to definitively determine in cases of doubt whether a DNA component was present or not (59).

This examination (Table 1) revealed that only AbMV DNA A was able to promote systemic infection by using leaf infiltration. The infection rate was lower than that observed after prick inoculation of stems, which generally approaches 100% for this virus-host combination in our hands. Interestingly, the expression of HA:AC1 alone was even more efficient than that of AbMV DNA A and revealed more reproducible titers in locally infected leaves throughout all treatments. HA:AC2 downregulated this effect again and led to a more stochastic appearance of viral DNA as well as a significant reduction in the amount of DNA per sample (mean rank, 1; rate, 11/13) (Table 1). In contrast, the coexpression of myc:AC3 with HA:AC1 and HA:AC2 enhanced viral titers and mobilization rates (mean rank, 2; rate, 13/13) (Table 1). In addition, this combination yielded a more homogeneous appearance from plant to plant, as well as from experiment to experiment, than did the combination of HA:AC1 and HA:AC2.

Having confirmed the overall reducing effect on viral DNA accumulation of HA:AC2 as an indicator of replication, it was interesting to examine whether an influence on minichromosome structure as an indicator of transcription could be inferred. To achieve this, the relative distributions of viral DNA B forms in gels (Fig. 3b) and the positions of topoisomers with 11 to 13 nucleosomes in 2D gels were determined as described previously (42). As exemplified for a single sample hybridized first against a DNA B-specific probe and then after stripping the probe, the same blot for the DNA A-specific probe, DNA A, and DNA B showed a similar distribution of the topoisomers, with a maximum of 12 superhelical turns (12 nucleosomes). Corresponding evaluations were performed with all samples whenever cccDNA was detected in the blots. However, no reliable and reproducible shifts in the topoisomer distribution were observed when HA:AC1, HA:AC1 plus HA:AC2, and HA:AC1 plus HA:AC2 plus myc:AC3 samples were compared (data not shown). In conclusion, we found no evidence for an influence of HA:AC2 on the condensation of AbMV minichromosomes, which would have reflected a function in transcription in this assay.

Another difference is worth mentioning. Only low levels of linear DNA were detectable in viral DNA B after AbMV DNA A inoculation (Fig. 3a and b), indicating that the extraction procedure is efficient and prevents nicking during DNA isolation. However, the overexpression of HA:AC1 alone or together with HA:AC2 and myc:AC3 led to a substantial increase in the level of a linear DNA species albeit smaller than genomic size (Fig. 3a, asterisk). More Rep protein in the cell may shift the equilibrium between nicking and closing reactions, leaving more linear ssDNA for complementary-strand replication (CSR) and, in consequence, incomplete replication products. In a normal infection, the production of such linear double-stranded DNA (dsDNA) would be a dead end of replication, which can be rescued only by RDR, as discussed in detail recently (46).

Replicational and transcriptional control in GFPexpress plants. To simplify the assay further by omitting the effects of the BC1 and BV1 proteins, as well as to easily monitor expression, transgenic GFPexpress plants with a duplication of the AbMV intergenic region were engineered in a way similar to that de-

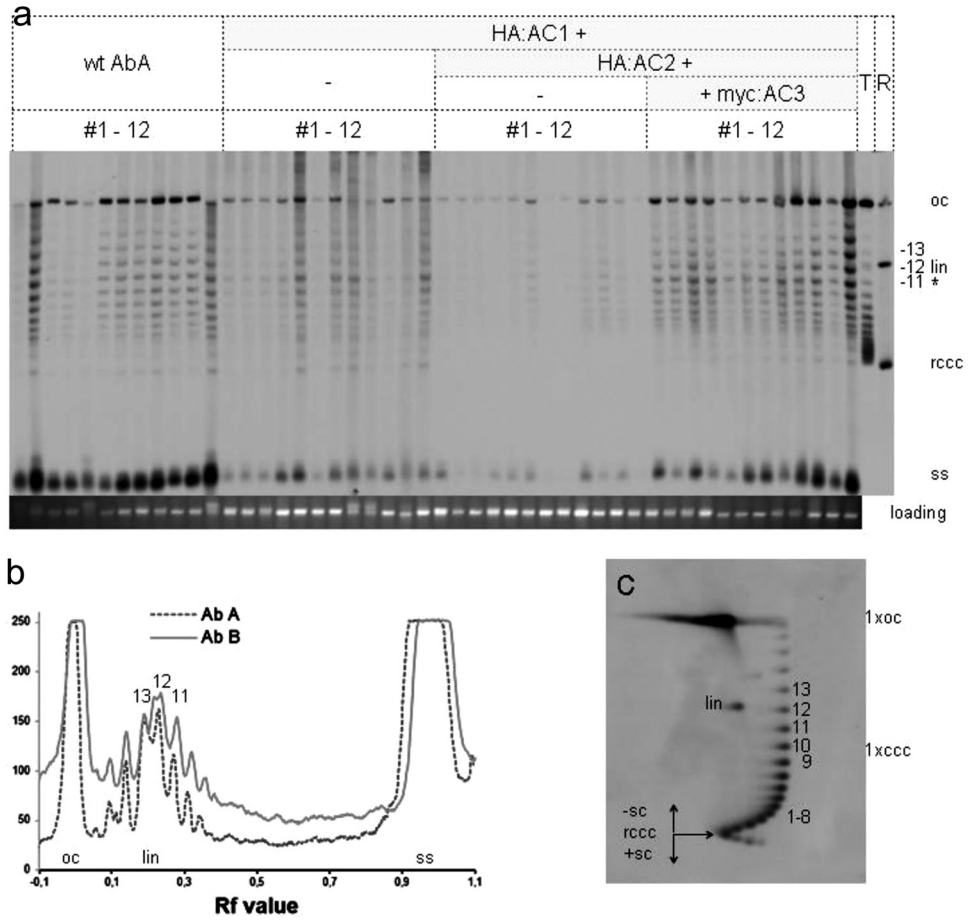

FIG 3 (a) Local agroinfiltration of transgenic DNA B plant leaves at 5 dpi, with wt AbMV DNA A (wt AbA) or HA:AC1-, HA:AC2-, or myc:AC3-expressing plasmids in the indicated combinations. Twelve independent leaf samples (samples 1 to 12) are shown for each treatment. Note the more prominent appearance of a linear dsDNA (asterisk) form that is smaller than the genomic linear DNA (lin) in samples treated with either HA:AC1 alone or a combination of HA:AC1, HA:AC2, and myc:AC3. In total nucleic acid extracts, viral DNAs were separated in chloroquine (10 μg/ml)-containing gels and detected by Southern blot hybridization using an AbMV DNA B probe. Lanes T and R are marker lanes with rcccDNA and topoisomer standards that indicate rcccDNA, linear DNA, and ocDNA positions. For comparison, aliquots of the samples were loaded onto an agarose gel without chloroquine, and the separated genomic host DNA was stained with ethidium bromide to judge loading. (b and c) Densitometry of a single lane of wt AbA, which was first hybridized against a DNA B-specific probe and subsequently hybridized, after stripping, with a DNA A-specific probe to demonstrate the similar distribution of DNA A and DNA B topoisomers with a maximum of 12 superhelical turns per molecule (12 nucleosomes per minichromosome) (b), as inferred from a 2D separation of a DNA B topoisomer standard (c).

scribed previously for tomato yellow leaf curl Sardinia virus (TYLCSV) (Fig. 1) (58).

The GFPexpress plants (3rd transgenic generation [T3]) tested positive for the transgene by mGFP4-specific PCR as well as by showing a low level of evenly distributed GFP fluorescence in leaves under UV light (data not shown). wt AbMV agroinfection of GFPexpress plants with both DNA components yielded systemic infection at 20 dpi with symptoms typical of AbMV infection of wt plants (37). Enhanced bright GFP fluorescence was detected in single cells of the vascular bundle (phloem companion cells) in GFPexpress plants (Fig. 4a), as expected for phloem-limited AbMV (37). RCA/RFLP (EcoRI) detection of circular DNA of systemically infected leaves exhibited the expected pattern for full-length DNA A (1,823 bp, 809 bp, and no cut in DNA B) (Fig. 4b), but the fragment expected for the transreplicon (2,890 bp) was not detectable under these conditions. These first control experiments confirmed that transgenic GFPexpress plants behave like wt hosts and do not interfere with any functions of AbMV.

Having established the principal functionality of the reporter plant line, the following experiments focused on local infection/inoculation for comparison with the results described above. In the first experimental setup, two leaves of two independent plants were each infiltrated twice, on the left and right sides, with the same constructs (Fig. 5). HA:AC1 was again sufficient to mobilize the GFPexpress replicon upon agroinfiltration. Increased GFP fluorescence levels were detected at between 2 and 6 dpi in all HA:AC1-infiltrated leaves (Fig. 5a and b). At later stages, this effect was enhanced by the coexpression of the gene silencing suppressor P19 (6 dpi) (Fig. 5b). Agroinfiltration of AbMV DNA A (AbA) (Fig. 5) revealed a fluorescence enhancement similar to that for HA:AC1 at 2 dpi but which was less efficient later on (6 dpi). An equivalent blocking of the HA:AC1 effect was induced by coinfiltration of an HA:AC2-expressing plasmid (HA:AC1 plus HA:AC2) (Fig. 5). Mock infiltration did not increase GFP fluorescence, excluding an effect of agrobacteria on expression.

The increase of GFP expression correlated with the production of GFPexpress replicons, as detected by an accumulation of the diagnostic fragment by RCA/RFLP (EcoRI), which monitors the

TABLE 1 Mobilization of DNA B in transgenic DNA B plants upon treatment with DNA A or after transient expression of viral proteins AC1, AC2, and AC3[a]

Treatment	Rank score																						No. of plants with mobilized DNA B/no. of inoculated plants
	Expt 1								Expt 2								Expt 3				Expt 4				Mean		
	L plant sample				S plant sample				L plant sample				S plant sample				L plant sample		S plant sample		L plant sample				S plant sample					
	1	2	3	4	1	2	3	4	1	2	3	4	1	2	3	4	1	2	1	2	1	2	3	4	1	2	3	4	L	S	L	S
AbA	4	4	4	4	4	4	4	4	0	3	0	0	0	0	0	0	3	3	4	4	0	0	0	0	0	0	0	0	2	1	7/14	6/14
HA:AC1	3	3	3	3	0	0	0	ND	4	4	4	4	0	0	0	0	4	4	0	0	4	4	4	4	0	0	0	0	3	0	14/14	0/13
HA:AC1 + HA:AC2	2	2	1	1	0	0	0	0	1	ND	1	1	0	0	0	0	1	1	0	0	1	1	1	1	0	0	0	0	1	0	11/13	0/14
HA:AC1 + HA:AC2 + myc:AC3	1	1	2	ND	0	0	0	0	2	2	2	2	0	0	0	0	2	2	0	0	2	2	2	2	0	0	0	0	2	0	13/13	0/14

[a] Shown are total signal intensities in rank scores per inoculation and plant sample. Rankings of Southern blot signals (0 to 4) are summarized, with 0 indicating no signal and 4 indicating the strongest signal. ND, not determined; L, local; S, systemic; AbA, transgenic DNA B plants upon treatment with DNA A.

FIG 4 Systemic agroinfection of GFPexpress plants with wt AbMV. (a) GFP fluorescence after transreplication in the phloem (P) in a hand-drawn cross section along a major vein detected by microscopy under UV light. White arrowheads mark GFP-expressing cells, blue fluorescence appeared in xylem elements (X). Bar, 100 μm. (b) Six independent samples from systemically infected plants at 14 dpi were analyzed by RCA/RFLP (EcoRI) analysis. Fragments were separated on a 1% agarose gel and stained with ethidium bromide afterwards, which showed the expected fragment sizes (bp) and some undigested (ud) DNA. M indicates PstI-digested lambda DNA as a molecular marker. m, mock-inoculated plants. Note that the concentration of the transreplicon (2,890 bp) was too low to be detected by the RCA/RFLP assay under these conditions.

generation of circular DNA progenitor molecules (2,890 bp) (Fig. 5c). Interestingly, transreplicon levels were significantly lower in AbA-infiltrated leaves than in HA:AC1-infiltrated ones, whereas additional P19 expression promoted transreplication. Even more pronounced was the repression of transreplication upon coexpression with HA:AC2.

These results support further the notion that HA:AC2 suppresses primarily replication in the context of viral DNA A as well as during its individual overexpression in this assay.

In a second experimental setup, the different plasmids were inoculated on the same leaves to reduce leaf-to-leaf variation (Fig. 6). The relevant proteins as well as small interfering RNAs (siRNAs) directed against GFP were detected by immunodetection or Northern blot hybridization, respectively (Fig. 6c). Note

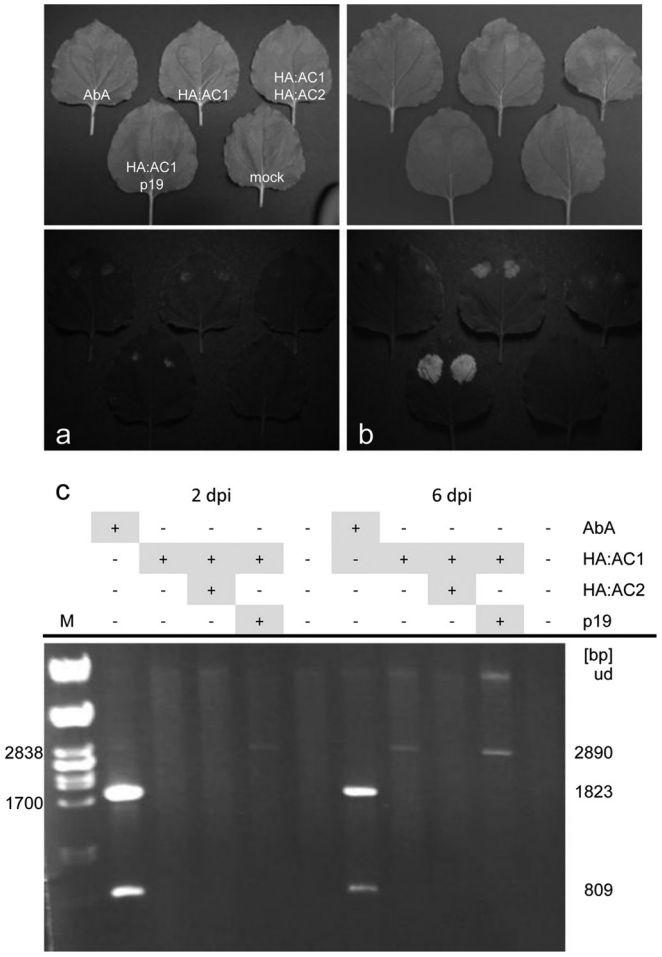

FIG 5 Local agroinfiltration on separate leaves of GFPexpress plants with wt AbMV DNA A (AbA), pPCV812-Menchu-Rep (HA:AC1), pPCV812-Menchu-TrAP(HA:AC2), or pBINp19 (P19) in different combinations, as indicated (48). (a and b) Samples at 2 dpi (a) or 6 dpi (b) under daylight (top) or UV light (bottom). (c) RCA/RFLP (EcoRI) detection of the corresponding plant samples as described in the legend of Fig. 4. Note the differential appearance of the diagnostic fragment (2,890 bp) for the transreplicon.

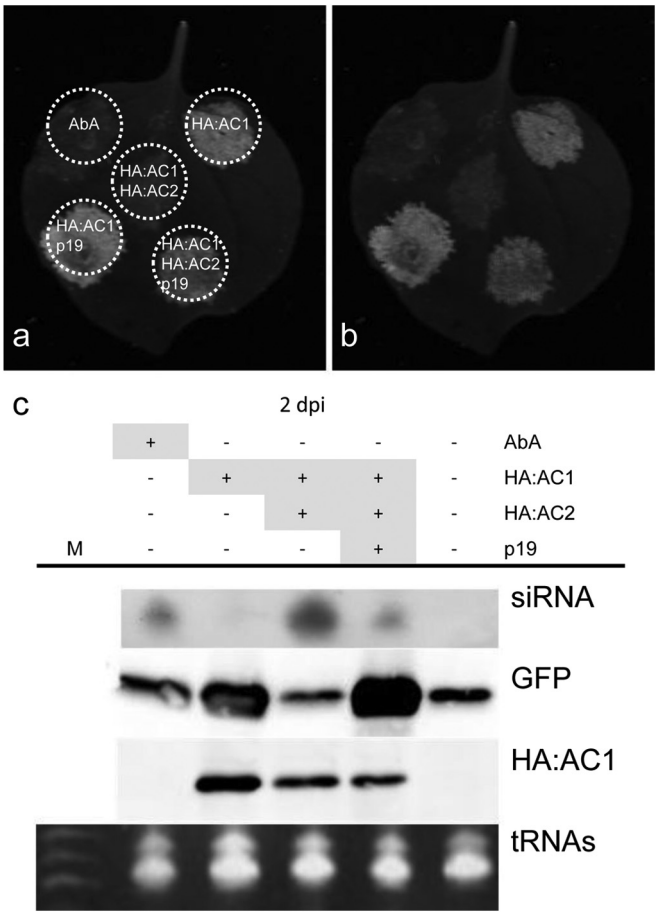

FIG 6 Local agroinfiltration as described in the legend of Fig. 5 but on the same leaf and monitored at 5 dpi. (a) Positions of inoculation. (b) GFP fluorescence. (c) Detection of relevant components after application of the same combination of constructs by Northern blot hybridization for GFP-specific siRNA or by immunodetection of GFP or of HA:AC1 by Western blotting with antiserum against GFP or HA, respectively. tRNAs served as a loading control after ethidium bromide staining. Lane M, 50-bp ladder (Fermentas).

that the construct pPCV812-Menchu-Rep expresses the target protein as an N-terminal HA-tagged splicing-dependent fusion product to exclude the detection of Rep, which might have been produced in the agrobacteria.

Similarly to the results described above, GFP fluorescence was enhanced by HA:AC1 expression and even more so in the presence of P19, and this effect was reversed if AC2 was present on wt AbA or individually as HA:AC2. Corresponding changes of GFP levels were detected by Western blotting (Fig. 6c), excluding a mere effect on the fluorescence activity of GFP by quenching. A small reduction of the protein levels for HA:AC1 was observed in the presence of HA:AC2, even if coexpressed with P19, which, however, was not sufficient to account for the changes in replication. Most prominent, however, was the increase of GFP siRNA levels (Fig. 6c) in the presence of HA:AC2, which was compensated for by the coexpression of P19. Infiltrations with either HA:AC2 or P19 alone did not increase GFP fluorescence under these conditions, confirming the necessity of transreplication (data not shown).

Modes of replication and minichromosome structure in GFPexpress plants. In order to discriminate between different modes of viral replication, as well as changes in minichromosome structure as an indicator of effects on transcription, GFPexpress plants were inoculated with HA:AC1- and HA:AC2-expressing plasmids, and the results were compared to those after wt DNA A infiltration.

To cope with plant-to-plant and experiment-to-experiment variation, five independent experimental sets with parallel treatments, including four biological replicates for each treatment, were performed. Blots are shown as representative examples, and the whole data set was evaluated by using the rank-numbering approach described above (Table 2). Total DNAs were prepared from the agroinfiltrated fluorescent areas and separated on 1D gels, and transreplicon DNA was detected by a GFP-selective probe with a short cross-hybridizing region of the AbMV common region for Southern blot hybridization, followed by densitometric analysis as described above.

Figure 7a exemplifies the results for one replicate. To relate the changes in topoisomer distributions to minichromosome struc-

TABLE 2 Transreplication in GFPExpress plants after local agroinfiltration with HA-tagged AC1 and AC2 or P19 in different combinations

Expt	Leaf	Rank score for treatment[a]			
		HA:AC1	HA:AC1 + HA:AC2	HA:AC1 + P19	HA:AC1 + HA:AC2 + P19
1	1	3	1	4	2
	2	3	1	4	2
	3	3	1	4	2
	4	3	1	4	2
2	1	3	1	4	2
	2	3	1	4	2
	3	3	1	4	2
	4	3	2	4	1
3	1	3	1	4	2
	2	3	1	4	2
	3	4	1	1	3
	4	3	1	4	2
4	1	3	2	4	1
	2	3	1	4	2
	3	3	1	4	2
	4	3	1	4	2
5	1	3	1	4	2
	2	3	1	4	2
	3	3	1	4	2
	4	3	1	4	2
Mean[b]		3.1	1.1	3.9	2.0
SD		0.2	0.3	0.7	0.4

[a] Shown are the total signal intensities in rank scores per treatment and plant sample. Rankings of the strength of Southern blot signals (scores of 1 to 4) are summarized, with 1 indicating the weakest signal and 4 indicating the strongest signal.
[b] A Wilcoxon signed-rank test indicated statistically significant differences between all treatments ($P < 0.001$).

ture, an appropriate topoisomer standard for the GFPexpress transreplicon (Fig. 7b) was separated on a 2D gel and hybridized. As for the other topoisomer standards, linear DNA migrated between cccDNA with 12 and 13 superhelical turns corresponding to 12 or 13 nucleosomes per minichromosome, in spite of the slightly larger size of this construct than that of wt AbMV DNAs. For wt DNA A treatment (AbA) (Fig. 7a), the DNA A pattern of bands was visible due to the cross-reacting probe, whereas the GFPexpress transreplicon was hardly visible. In comparison with this lane, the other treatments showed the expected shift of bands to lower mobility on account of the larger size of the transreplicon. HA:AC1 alone was sufficient to transreplicate the reporter, and this construct was even more efficient than AbA alone. HA:AC2 repressed this effect in combination with HA:AC1 alone as well as when HA:AC1 and P19 were coinfiltrated. P19 promoted HA:AC1-dependent transreplication significantly (Fig. 7c) but only partially compensated for the decreasing effect of HA:AC2.

This individual result was reproduced in five independent experimental sets, with all treatments always in parallel (Fig. 7c).

Densitometric analyses of all lanes were performed, and the maxima of the topoisomer distributions were evaluated, which did not show any significant reproducible differences between treatments (data not shown).

An artifact in the interpretation of the hybridization results described above is possible due to the complex replication strategies of geminiviruses. It is possible, particularly for the RDR mode, that the lack of cccDNA bands is erroneously interpreted because molecules engaged in this replication pathway (cccDNA and heterogeneous linear dsDNA or ssDNA) could transform discrete bands into a smear with a corresponding reduction of signal intensity. To investigate this possibility, samples were treated with exonuclease V (also known as RecBCD) before separation of the DNA on 1D chloroquine-agarose gels (Fig. 8). This pretreatment removes all linear DNA and should liberate the cccDNA engaged in replicative intermediates. However, the results were the same as those described above (Fig. 8): HA:AC2 reduced the amount of cccDNA considerably in all variants tested and in parallel samples, independent of P19 action.

Effects on DNA methylation. As the AC2 protein has been shown to change the methylation of DNA, additional experiments were designed to determine whether the methylation of the transreplicon might be changed. Applying the methylation-dependent restriction enzyme McrBC as described recently (41), DNAs were treated with or without McrBC and analyzed by hybridization as described above (Fig. 9). This enzyme recognizes (G/A)mC(N40-3000). AbMV DNA A contains 137 GC and 126 AC sites, and DNA B contains 108 GC and 138 AC sites, which are distributed over the whole genome; thus, many possible sites are cleavable. If AC2 decreased methylation by interfering with the methyl cycle, the remaining cccDNA should be more resistant to McrBC in these samples. Confirming previous results (41), multimeric DNA was preferentially reduced, and amounts of monomeric linear dsDNA increased selectively after enzyme treatment (Fig. 9). However, the overexpression of HA:AC2 did not prevent this digestion and showed a decrease in the level of viral multimeric DNA as well as the appearance of the characteristic linear DNA. These results do not support a reduced methylation of viral DNA by AbMV AC2 in this assay.

Detection of AC2 proteins. The detection of AC2 proteins in plants is a challenge. So far, AC2 proteins have been investigated by using samples expressed ectopically *in vitro* (64), in insect cells (17), or in bacteria (18, 50, 65). Most authors have observed an anomalous migration behavior of the respective proteins. For TGMV AC2 (17), this was thought to be caused by phosphorylation. However, AbMV AC2 showed the same aberrant migration when expressed in *E. coli* (50) but yielded no phosphate signals after metabolic labeling, in contrast to other geminiviral proteins in the same study. To further explore this issue, we separated the enriched, bacterially produced AbMV AC2 protein in two-dimensional PA gels (Fig. 10) and determined its apparent molecular weight in comparison to its isoelectric point (pI). The results show that AbMV AC2 migrated according to the calculated pI of 8.35 (Fig. 10b) but with an observed apparent molecular weight of 23.2 (Fig. 10c), in comparison to the calculated molecular mass of 14.6 kDa. Therefore, it is likely that AbMV AC2 migrates abnormally despite the absence of posttranslational modifications that change the charge substantially, such as phosphorylation.

In order to explore whether the charge of AbMV AC2 is special compared to those of distinct homologous gene products, the pI values of the 964 next relatives along with their calculated molecular weights were determined (Fig. 10d and e). A remarkable variability in the respective pIs among individual geminiviruses was detected, with several discrete peaks (Fig. 10d) and clustering with

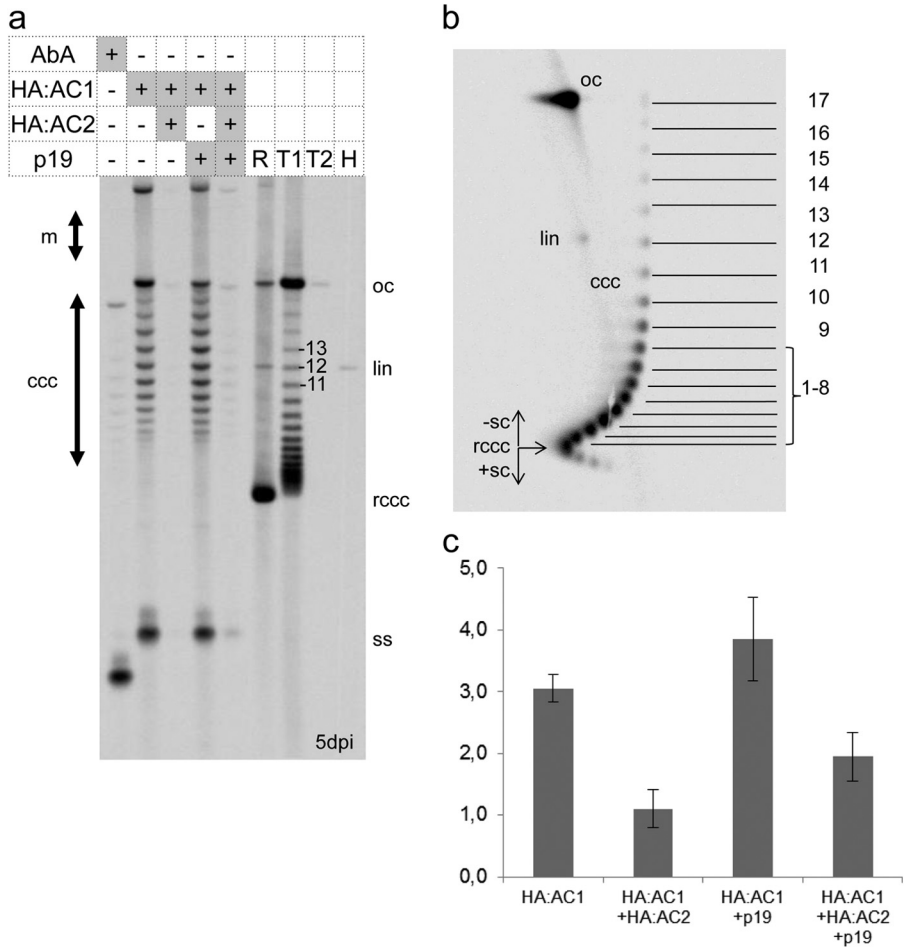

FIG 7 Viral DNA forms in agroinfiltrated GFPexpress plants at 5 dpi. (a) Example of each treatment as described in the legend of Fig. 3. Samples were separated on a 1.4% agarose gel supplemented with 10 μg/ml chloroquine and hybridized with a GFP probe. The indicated DNA forms are described in the legend of Fig. 3. Standards are relaxed covalently closed circular DNA (R); topoisomer standards (T1 and T2) with increasing topoisomer density from bottom to top, as determined by 2D gel electrophoresis; and a linear hybridization standard (H). (b) Topoisomer distribution of the transreplicon GFPexpress standard (rcccDNA after gyrase treatment) after 2D agarose gel electrophoresis and hybridization with a GFP probe. DNA forms are indicated as described in the legend of Fig. 2 and in the directions of increasing negative (−sc) or positive (+sc) superhelicity. Gel conditions in the first dimension were 0.3% SDS for 22 h at 10 V, and those in the second dimension were 10 μg/ml chloroquine for 22 h at 45 V. (c) Bar chart of the rank-numbering approach. Viral titers of the GFP transreplicon of samples such as those in panel a were ordered by rank numbers (where 1 indicates the weakest signal and 4 indicates the strongest signal) for 5 independent experimental sets with parallel treatments, including four biological replicates. The Wilcoxon signed-rank test showed a statistically significant difference for all treatments (Table 2).

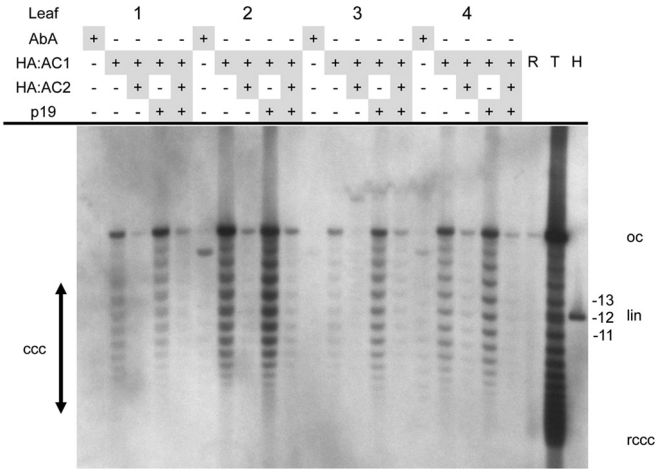

FIG 8 Separation of samples such as those described in the legend of Fig. 7 but pretreated with exonuclease V.

respect to the corresponding molecular weights (Fig. 10b). When the pIs of the AbMV (8.35) and TGMV (9.33) AC2 proteins are compared, they represent opposite examples from the borders of the distribution. Screening of these values for correlations with geographic or host species origins did not reveal any obvious relationship.

In comparison to other geminiviral proteins, it was difficult to produce large amounts of AbMV AC2 in bacteria, but complementation with a plasmid encoding a tRNA for rare arginine codons improved the yield to some extent (50). Similarly, the detection of AbMV AC2 in plants was a greater challenge. Using an anti-AbMV AC2 antibody raised against bacterially produced and purified protein (50), the best of what we could see in Western blots is shown in Fig. 11a (asterisks) for systemically infected plant tissues. To the best of our knowledge, these results show for the first time the respective (A)C2-specific bands unequivocally in plants. The main, upper band shows the aberrant migration be-

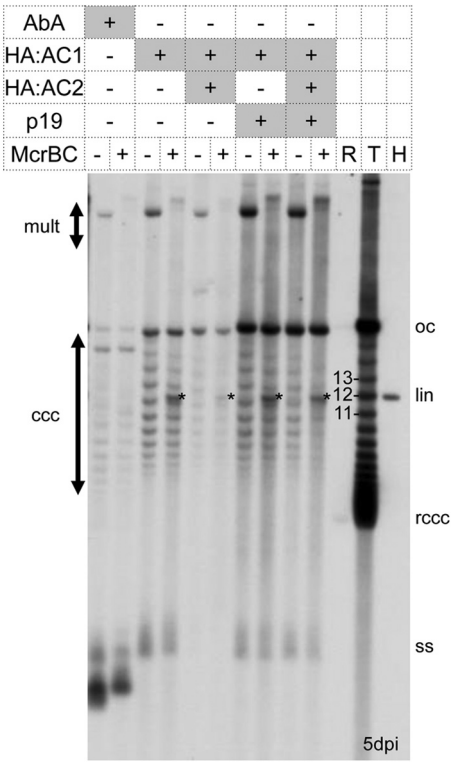

FIG 9 Methylation-dependent restriction analysis. Samples as described in the legend of Fig. 7 were treated with (+) or without (−) McrBC prior to separation on a 1.4% agarose gel containing 10 μg/ml chloroquine, Southern blot hybridization, and detection with a GFP probe. DNA forms and standards are described in the legend of Fig. 7; asterisks indicate possible additional linear DNAs after enzyme digestion.

havior known for bacterially expressed proteins. In addition, a minor, lower band migrated close to the expected value. In spite of extensive efforts, we were unable to detect the locally expressed AC2 proteins, with or without an HA tag, reliably by the antibody directed against the cognate AbMV AC2 (Fig. 11a, local, and data not shown). In contrast, at least some HA:AC2 protein was detectable unequivocally by using an anti-HA antibody (Fig. 11b), preferentially in pellet fractions when expressed alone or in total protein extracts when expressed together with HA:AC1. The strong difference in signal intensities between HA:AC1 and HA:AC2 (Fig. 11b) revealed that the proteins were differentially expressed or had differing stabilities in plants to a considerable degree.

Translation of AC2 is necessary for the brake effect. It is possible to consider whether the observed effect of the HA:AC2 construct was caused by either the additional 35S promoter or the transcript alone. Both scenarios have been excluded by a control experiment with a further construct without the ability to translate AC2 sequences (HA:AC2fs) (Fig. 11c). A −1 frameshift mutation was created to retain the HA and intron sequences to yield the most comparable transcription, with HA fused to the C-terminal sequence of the overlapping AC1 gene instead of the AC2 gene. This construct did not interfere with HA:AC1-dependent replication (Fig. 11c).

DISCUSSION

Like Columbus, we went out to search for changes in viral minichromosome architecture due to AC2 but discovered a completely new function in replication. To ensure that this novel finding is reliable, the experiments were repeated several times and replicated by two independent researchers. This led to the conclusion that, at least for AbMV AC2 and the chosen assay conditions, this protein downregulates viral replication. In contrast, no reproducible change in minichromosome condensation was detectable. In addition, AbMV AC2 enhanced posttranscriptional gene silencing (PTGS), rather than suppressing it, in a special assay using GFPexpress plants. This result is consistent with the known functions of AC2 as a transcriptional activator, since the artificial replicon contains the strong 35S promoter in an orientation opposite that of the AbMV AV1 promoter. Upon the activation of the AV1 promoter by AC2, bidirectional transcriptional collisions may occur, which may result in enhanced siRNA generation (4). The two functions in replication suppression and PTGS enhancement appeared to be unconnected, as the level of Rep was not reduced considerably in the presence of AC2, and AC3 did not increase Rep levels, although it reversed the AC2 effect on replication. Therefore, a third function must be responsible for replication suppression, possibly on the basis of host counterdefense.

Although at first glance surprising, the conserved genomic organization of AC1, AC2, and AC3 with overlapping ORFs may reflect just a concerted action in replication regulation. A stringent control of geminiviral replication in host tissues may be advantageous for the virus. The overexpression of Rep has been shown to induce the rereplication of host DNA in yeast (66, 67), and geminiviral infection led to the same effect on plants (68), in addition to enhanced somatic homologous recombination (69). It is likely that these detrimental effects need to be minimized in order to optimize viral fitness. Moreover, the overexpression of Rep yielded more defective linear DNA molecules upon the transreplication of DNA B in this study (Fig. 3). In order to avoid these unproductive DNAs, the transcription of AC1 may be reduced by autorepression, as described previously (70–72).

Indirect causes for the biological functions of AC2 have to be taken into account. The overexpression of TYLCV-C C2 from a potato virus X (PVX) vector induced substantial necrosis in *N. benthamiana* plants (19), although necrotic symptoms are rarely observed for geminiviruses. For the samples documented in this study, necrosis was rarely detected macroscopically. In order to examine whether a subtle necrotic response may be a cause of reduced replication, the yields of DNA per leaf sample were compared, and no significant differences between samples with and those without AC2 were observed (data not shown). The detection of high levels of Rep protein (Fig. 6) in the samples lends further support to the conclusion that necrosis is not the key factor in the chosen assays.

Nevertheless, the potential of C2 to elicit a host response may be key to understanding the function of C2 as an avirulence gene. This view has been elucidated by the to-date-unique, but economically important, case (73) of cotton leaf curl Burewala virus (CLCuBuV). This virus has broken resistance in cotton by developing distinct isolates in Pakistan with mutated C2 genes. Frameshift or premature stop mutants allow the expression of only a truncated version of C2 without a transactivation domain. The authors of that study proposed an avirulence function of C2. In this context, it is worth noting that most knowledge about the transactivation function of (A)C2 is based on the analysis of bipartite begomoviruses, whereas results for monopartite begomoviruses are scarce (74, 75).

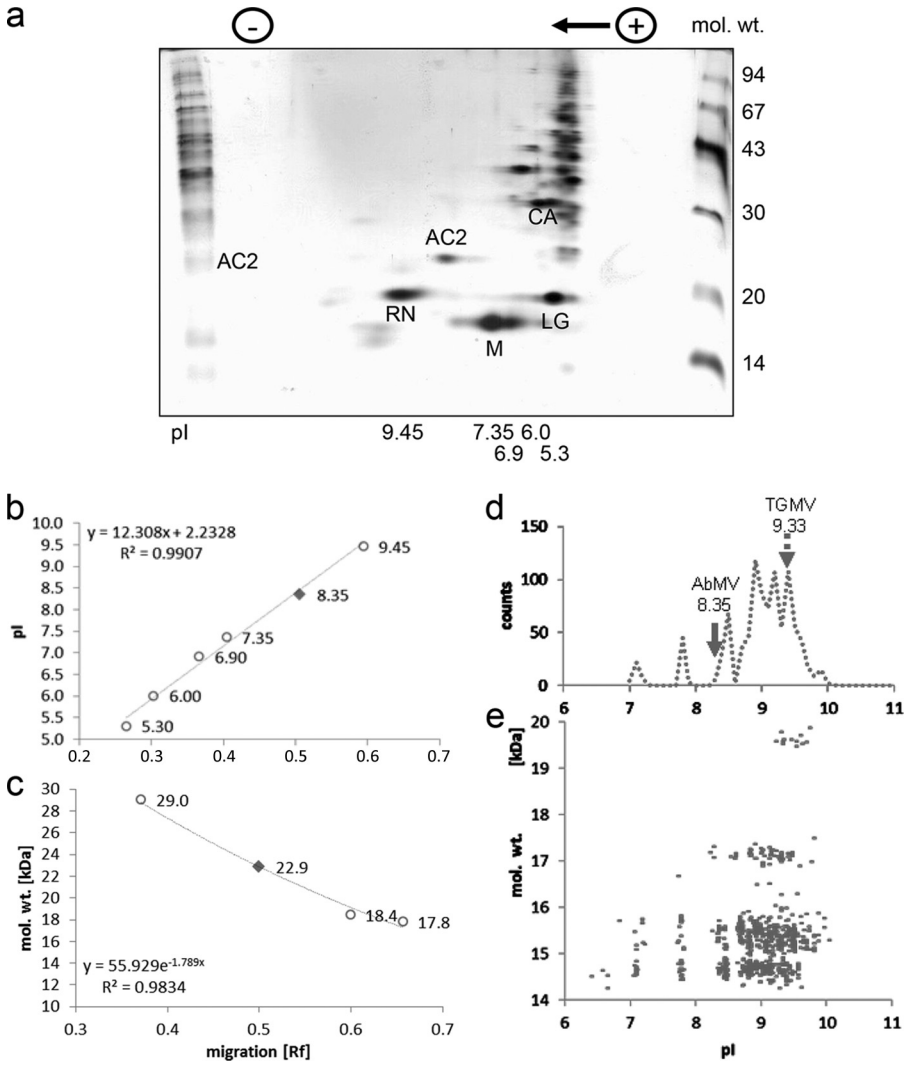

FIG 10 AC2 protein properties. (a) Determination of AbMV AC2 pI and apparent molecular weight by two-dimensional acrylamide gel electrophoresis (silver staining). Shown are data for first-dimension NEPHGE and second-dimension SDS-PAGE with the marker proteins RNase (RN), myoglobin (M), carbonic anhydrase (CA), and lactoglobulin (LG). For comparison, total bacterial input proteins were loaded in a separate lane (left) and with molecular weight standards (right). (b and c) Evaluation of this gel was performed, with marker spots indicated by circles and AC2 indicated by diamond for pI (b) and molecular weight (in thousands) (c). Equations define the best-fit curves with a goodness-of-fit test by Pearson's correlation coefficient. (d and e) The 964 next begomovirus relatives of AbMV AC2 were retrieved from Swiss-Prot, and their theoretical molecular weights as well as pIs were determined by using the ExPasy Web tool, with frequency distributions (d) and relationships between molecular weights and pIs (e) shown. For orientation, the respective positions of AbMV-WI AC2 and TGMV AC2 are indicated (arrows). Migration from left to right or from top to bottom in panel a is plotted as relative values (R_f).

A multitude of (A)C2 effects on host cell physiology is likely and is supported by data from protein-protein interaction assays (20, 23–25) and transcriptomic analyses (26–28) and the documentation of detrimental effects upon transgenic plant expression (32). Since some very basal host enzymes may be inhibited by (A)C2, pleiotropic effects are not unexpected and may explain the reduced replication of the indicator replicon in this study.

Nevertheless, direct effects are therefore not excluded. AC2 has been described as a sequence-nonspecific DNA binding protein. Although mainly its ssDNA binding activity is generally referred to, dsDNA binding has been found to different degrees for TGMV and potato yellow mosaic virus in the original literature (17, 65). The DNA binding capacity and the zinc finger motif of AC2 (17) may block efficient CSR, RCR, and/or RDR. The strength of this binding may be influenced by the charge of the protein, and the broad variation of the pI value (Fig. 10d and e) may suggest why different viruses exhibit different results for DNA binding. The charge parameter can be further modulated by posttranscriptional modifications such as phosphorylation. Interestingly, Shen et al. (18) found a differential phosphorylation of AC2 by SnRK, a signaling kinase involved in regulating sugar metabolism (76, 77), dependent on the geminivirus species. This implies a change of the AC2 charge in the dependence of the carbohydrate level and a fine-tuning of its effect on replication.

A further level of virus-specific AC2 regulation is its expression efficiency and/or its stability in the host. Transcriptional gene silencing (TGS) and PTGS have to be considered. As was shown previously for other geminiviral proteins (78–80), the coexpression of a PTGS suppressor such as P19 may enhance protein yield, a prerequisite which was also important for AbMV AC2 in this

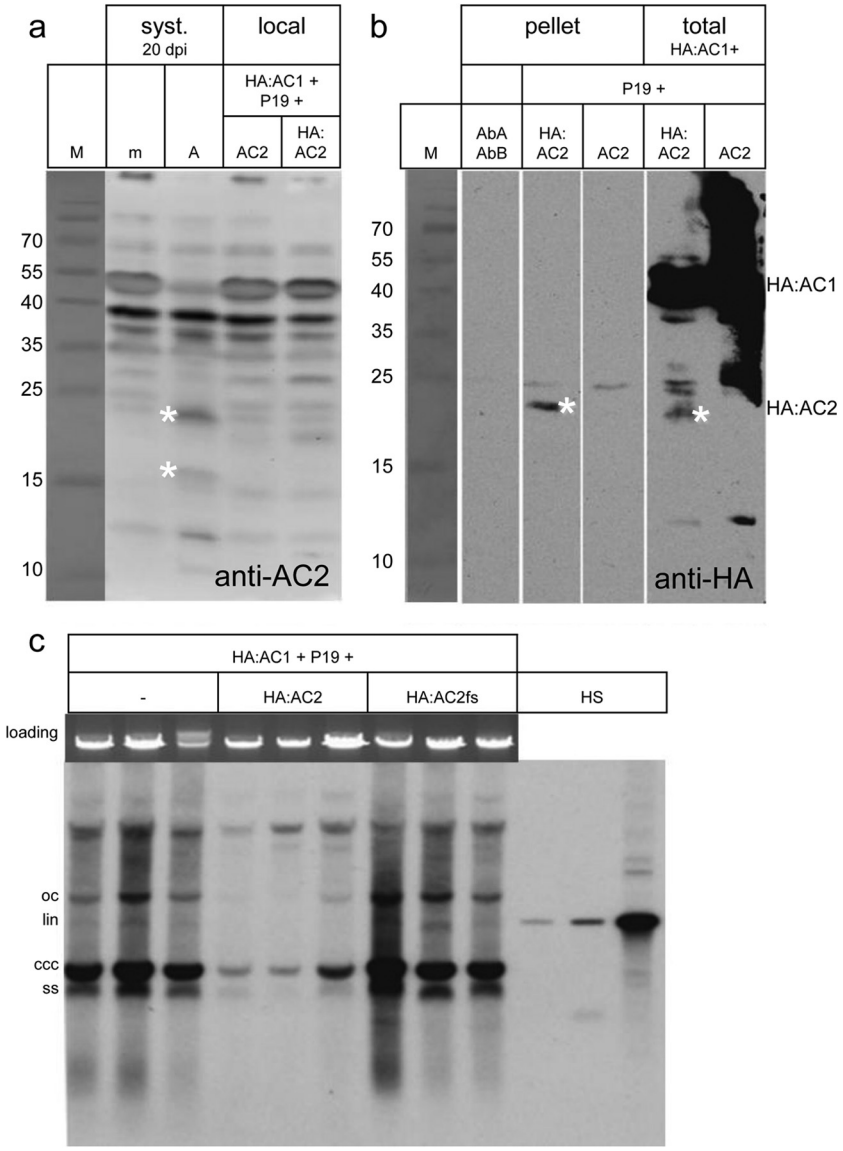

FIG 11 *In planta* detection of the AbMV-WI AC2 protein and translation control. (a and b) Western blots of 1D SDS-PAGE using anti-AC2 antibodies (a) or anti-HA antibodies (b) with reference to prestained marker proteins in the same blots. Molecular weight is indicated (in thousands). Asterisks indicate possible AC2-specific bands. m, mock-inoculated plants; A, AbMV-infected plants harvested at 20 dpi; local, agroinfiltration experiments at 5 dpi with the indicated combinations of expression constructs; M, marker. (c) Agroinfiltration at 5 dpi confirms the brake effect of HA:AC2 only if the AC2 sequence was translated. In addition to the constructs described above, a frameshift mutant (HA:AC2fs) was tested in parallel, and the total DNAs from each treatment (in triplicates of independent plants) are compared after hybridization with an AbMV A-specific probe after DNAs were separated on a 1% agarose gel containing 0.5 μg/ml ethidium bromide. The loading control is plant genomic DNA of the same sample and gel; HS is the hybridization standard for 1, 10, and 100 pg.

study. Placing an intron into the gene of interest may additionally reduce PTGS effects (81). A TGS effect of multiple 35S promoters on different plasmid constructs is also conceivable, but we did not observe any such effect in our agroinfiltration experiments. Even the application of a third 35S promoter in the case of HA:AC3 expression experiments did not reduce replication. Taking into consideration the additional improvement by P19 expression from a further 35S promoter, a role of TGS at this stage of inoculation is less likely. A further control experiment with a frameshift mutant of HA:AC2 completely excluded promoter and RNA effects as the relevant causes. Although AC2 expression was improved by the avoidance of PTGS, the level of protein was still very low, an experience which was also mentioned recently by other authors (18). Therefore, we believe that this is a more general problem, which is solved for the first time in this study. Detection reactions with our anti-AC2 antibody (50) have to be developed to such an extent that numerous cross-reacting host proteins appear. Nevertheless, the specific signals can be discriminated (Fig. 11), and thereby, the host proteins can be used as a loading control. The anti-HA antibody reaction, which is usually strong and selective, as shown here for HA:AC1 and previously for other geminiviral proteins (53, 78–80, 82), supports the notion that the AC2 protein accumulates to very low levels (Fig. 11b), independently of whether HA:AC2 was expressed alone or together with HA:AC1. It

was difficult to detect the faint HA:AC2 signals against the background of the strong HA:AC1 signals in most of the many experiments done to solve this question. These results show that the use of an intron, an HA tag, and a silencing suppressor has paved the way to the detection of the AC2 protein for the first time.

Interestingly, the effect of AC2 was counteracted by AC3, explaining the well-known replication enhancer (REn) function of this protein in addition to the functions reported in previous studies (10, 83–86). How complex such an interaction might be, however, has been shown for *Beet curly top virus* (BCTV) C2, which promoted the replication of the unrelated monopartite begomovirus TYLCSV (28, 87).

Therefore, the role of AbMV AC2 as a replication brake is a novel add-on in the functional analysis of this pathogenicity factor. Possibly, this explanation is heuristic to understanding many of the secondary effects of AC2 as well. If not only viral replication but also host DNA replication was reduced, this would prevent rereplicating cells from entering mitosis at a later stage of virus multiplication.

ACKNOWLEDGMENTS

We thank Csaba Koncz (MPI for plant breeding, Cologne, Germany) for the binary vectors pPCV812-Menchu and pPCV002-Gigi, Dániel Silhavy and József Burgyán (Agricultural Biotechnology Center, Gödöllö, Hungary) for the P19 expression plasmid, Bruno Gronenborn and Katharina Hipp for helpful critical discussions, as well as Diether Gotthardt for taking care of the plants.

This research was supported by grants from the DFG (Je116/15-1) and the ERA-PG program (BMBF 0313986).

REFERENCES

1. **Varsani A, Navas-Castillo J, Moriones E, Hernandez-Zepeda C, Idris A, Brown JK, Murilo Zerbini F, Martin DP.** 2014. Establishment of three new genera in the family Geminiviridae: Becurtovirus, Eragrovirus and Turncurtovirus. Arch Virol **159:**2193–2203. http://dx.doi.org/10.1007/s00705-014-2050-2.
2. **Jeske H.** 2009. Geminiviruses, p 185–226. *In* zur Hausen H, de Villiers E-M (ed), Torque Teno virus: the still elusive human pathogens, vol 331. Springer, Berlin, Germany.
3. **Raja P, Wolf JN, Bisaro DM.** 2010. RNA silencing directed against geminiviruses: post-transcriptional and epigenetic components. Biochim Biophys Acta **1799:**337–351. http://dx.doi.org/10.1016/j.bbagrm.2010.01.004.
4. **Pooggin MM.** 2013. How can plant DNA viruses evade siRNA-directed DNA methylation and silencing? Int J Mol Sci **14:**15233–15259. http://dx.doi.org/10.3390/ijms140815233.
5. **Hanley-Bowdoin L, Bejarano ER, Robertson D, Mansoor S.** 2013. Geminiviruses: masters at redirecting and reprogramming plant processes. Nat Rev Microbiol **11:**777–788. http://dx.doi.org/10.1038/nrmicro3117.
6. **Sunter G, Hartitz MD, Hormuzdi SG, Brough CL, Bisaro DM.** 1990. Genetic analysis of tomato golden mosaic virus: ORF AL2 is required for coat protein accumulation while ORF AL3 is necessary for efficient DNA replication. Virology **179:**69–77. http://dx.doi.org/10.1016/0042-6822(90)90275-V.
7. **Sunter G, Bisaro DM.** 1991. Transactivation in a geminivirus: AL2 gene product is needed for coat protein expression. Virology **180:**416–419. http://dx.doi.org/10.1016/0042-6822(91)90049-H.
8. **Sunter G, Bisaro DM.** 1992. Transactivation of geminivirus AR1 and BR1 gene expression by the viral AL2 gene product occurs at the level of transcription. Plant Cell **4:**1321–1331. http://dx.doi.org/10.1105/tpc.4.10.1321.
9. **Sunter G, Hartitz MD, Bisaro DM.** 1993. Tomato golden mosaic virus leftward gene expression: autoregulation of geminivirus replication protein. Virology **195:**275–280. http://dx.doi.org/10.1006/viro.1993.1374.
10. **Sunter G, Stenger DC, Bisaro DM.** 1994. Heterologous complementation by geminivirus AL2 and AL3 genes. Virology **203:**203–210. http://dx.doi.org/10.1006/viro.1994.1477.
11. **Sunter G, Bisaro DM.** 1997. Regulation of a geminivirus coat protein promoter by AL2 protein (TrAP): evidence for activation and derepression mechanisms. Virology **232:**269–280. http://dx.doi.org/10.1006/viro.1997.8549.
12. **Sunter G, Sunter JL, Bisaro DM.** 2001. Plants expressing tomato golden mosaic virus AL2 or beet curly top virus L2 transgenes show enhanced susceptibility to infection by DNA and RNA viruses. Virology **285:**59–70. http://dx.doi.org/10.1006/viro.2001.0950.
13. **Yang X, Baliji S, Buchmann RC, Wang H, Lindbo JA, Sunter G, Bisaro DM.** 2007. Functional modulation of the geminivirus AL2 transcription factor and silencing suppressor by self-interaction. J Virol **81:**11972–11981. http://dx.doi.org/10.1128/JVI.00617-07.
14. **Lacatus G, Sunter G.** 2009. The Arabidopsis PEAPOD2 transcription factor interacts with geminivirus AL2 protein and the coat protein promoter. Virology **392:**196–202. http://dx.doi.org/10.1016/j.virol.2009.07.004.
15. **Berger MR, Sunter G.** 2013. Identification of sequences required for AL2-mediated activation of the tomato golden mosaic virus-yellow vein BR1 promoter. J Gen Virol **94:**1398–1406. http://dx.doi.org/10.1099/vir.0.050161-0.
16. **Hormuzdi SG, Bisaro DM.** 1995. Genetic analysis of beet curly top virus: examination of the roles of L2 and L3 genes in viral pathogenesis. Virology **206:**1044–1054. http://dx.doi.org/10.1006/viro.1995.1027.
17. **Hartitz MD, Sunter G, Bisaro DM.** 1999. The tomato golden mosaic virus transactivator (TrAP) is a single-stranded DNA and zinc-binding phosphoprotein with an acidic activation domain. Virology **263:**1–14. http://dx.doi.org/10.1006/viro.1999.9925.
18. **Shen W, Dallas MB, Goshe MB, Hanley-Bowdoin L.** 2014. SnRK1 phosphorylation of AL2 delays Cabbage leaf curl virus infection in Arabidopsis. J Virol **88:**10598–10612. http://dx.doi.org/10.1128/JVI.00761-14.
19. **van Wezel R, Liu H, Tien P, Stanley J, Hong Y.** 2001. Gene C2 of the monopartite geminivirus tomato yellow leaf curl virus-China encodes a pathogenicity determinant that is localized in the nucleus. Mol Plant Microbe Interact **14:**1125–1128. http://dx.doi.org/10.1094/MPMI.2001.14.9.1125.
20. **Wang H, Hao L, Shung CY, Sunter G, Bisaro DM.** 2003. Adenosine kinase is inactivated by geminivirus AL2 and L2 proteins. Plant Cell **15:**3020–3032. http://dx.doi.org/10.1105/tpc.015180.
21. **Yang XL, Xie Y, Raja P, Li SZ, Wolf JN, Shen QT, Bisaro DM, Zhou XP.** 2011. Suppression of methylation-mediated transcriptional gene silencing by beta C1-SAHH protein interaction during geminivirus-betasatellite infection. PLoS Pathog **7:**e1002329. http://dx.doi.org/10.1371/journal.ppat.1002329.
22. **Baliji S, Lacatus G, Sunter G.** 2010. The interaction between geminivirus pathogenicity proteins and adenosine kinase leads to increased expression of primary cytokinin-responsive genes. Virology **402:**238–247. http://dx.doi.org/10.1016/j.virol.2010.03.023.
23. **Buchmann RC, Asad S, Wolf JN, Mohannath G, Bisaro DM.** 2009. Geminivirus AL2 and L2 proteins suppress transcriptional gene silencing and cause genome-wide reductions in cytosine methylation. J Virol **83:**5005–5013. http://dx.doi.org/10.1128/JVI.01771-08.
24. **Wang H, Buckley KJ, Yang X, Buchmann RC, Bisaro DM.** 2005. Adenosine kinase inhibition and suppression of RNA silencing by geminivirus AL2 and L2 proteins. J Virol **79:**7410–7418. http://dx.doi.org/10.1128/JVI.79.12.7410-7418.2005.
25. **Hao L, Wang H, Sunter G, Bisaro DM.** 2003. Geminivirus AL2 and L2 proteins interact with and inactivate SNF1 kinase. Plant Cell **15:**1034–1048. http://dx.doi.org/10.1105/tpc.009530.
26. **Soitamo AJ, Jada B, Lehto K.** 2012. Expression of geminiviral AC2 RNA silencing suppressor changes sugar and jasmonate responsive gene expression in transgenic tobacco plants. BMC Plant Biol **12:**204–222. http://dx.doi.org/10.1186/1471-2229-12-204.
27. **Trinks D, Rajeswaran R, Shivaprasad PV, Akbergenov R, Oakeley EJ, Veluthambi K, Hohn T, Pooggin MM.** 2005. Suppression of RNA silencing by a geminivirus nuclear protein, AC2, correlates with transactivation of host genes. J Virol **79:**2517–2527. http://dx.doi.org/10.1128/JVI.79.4.2517-2527.2005.
28. **Caracuel Z, Lozano-Duran R, Huguet S, Arroyo-Mateos M, Rodriguez-Negrete EA, Bejarano ER.** 2012. C2 from beet curly top virus promotes a cell environment suitable for efficient replication of geminiviruses, pro-

viding a novel mechanism of viral synergism. New Phytol **194:**846–858. http://dx.doi.org/10.1111/j.1469-8137.2012.04080.x.
29. **Liu L, Chung H, Lacatus G, Baliji S, Ruan J, Sunter G.** 2014. Altered expression of Arabidopsis genes in response to a multifunctional geminivirus pathogenicity protein. BMC Plant Biol **14:**302. http://dx.doi.org/10.1186/s12870-014-0302-7.
30. **Chung HY, Sunter G.** 2014. Interaction between the transcription factor AtTIFY4B and begomovirus AL2 protein impacts pathogenicity. Plant Mol Biol **86:**185–200. http://dx.doi.org/10.1007/s11103-014-0222-9.
31. **Chung YH, Lacatus G, Sunter G.** 2014. Geminivirus AL2 protein induces expression of, and interacts with, a calmodulin-like gene, an endogenous regulator of gene silencing. Virology **460–461:**108–118. http://dx.doi.org/10.1016/j.virol.2014.04.034.
32. **Rahman J, Karjee S, Mukherjee SK.** 2012. MYMIV-AC2, a geminiviral RNAi suppressor protein, has potential to increase the transgene expression. Appl Biochem Biotechnol **167:**758–775. http://dx.doi.org/10.1007/s12010-012-9702-z.
33. **Wege C, Gotthardt RD, Frischmuth T, Jeske H.** 2000. Fulfilling Koch's postulates for Abutilon mosaic virus. Arch Virol **145:**2217–2225. http://dx.doi.org/10.1007/s007050070052.
34. **Fischer A, Strohmeier S, Krenz B, Jeske H.** Evolutionary liberties of the Abutilon mosaic virus cluster. Virus Genes, in press. http://dx.doi.org/10.1007/s11262-014-1125-1.
35. **Höhnle M, Höfer P, Bedford ID, Briddon RW, Markham PG, Frischmuth T.** 2001. Exchange of three amino acids in the coat protein results in efficient whitefly transmission of a nontransmissible Abutilon mosaic virus isolate. Virology **290:**164–171. http://dx.doi.org/10.1006/viro.2001.1140.
36. **Wege C, Siegmund D.** 2007. Synergism of a DNA and an RNA virus: enhanced tissue infiltration of the begomovirus Abutilon mosaic virus (AbMV) mediated by Cucumber mosaic virus (CMV). Virology **357:**10–28. http://dx.doi.org/10.1016/j.virol.2006.07.043.
37. **Wege C, Saunders K, Stanley J, Jeske H.** 2001. Comparative analysis of tissue tropism of bipartite geminiviruses. J Phytopathol **149:**359–368. http://dx.doi.org/10.1046/j.1439-0434.2001.00640.x.
38. **Wyant PS, Kober S, Schwierzok A, Kocher C, Schafer B, Jeske H, Wege C.** 2012. Cloned tomato golden mosaic virus back in tomatoes. Virus Res **167:**397–403. http://dx.doi.org/10.1016/j.virusres.2012.05.021.
39. **Evans D, Jeske H.** 1993. Complementation and recombination between mutants of complementary sense genes of DNA A of Abutilon mosaic virus. Virology **197:**492–496. http://dx.doi.org/10.1006/viro.1993.1619.
40. **Jeske H, Lütgemeier M, Preiss W.** 2001. Distinct DNA forms indicate rolling circle and recombination-dependent replication of Abutilon mosaic geminivirus. EMBO J **20:**6158–6167. http://dx.doi.org/10.1093/emboj/20.21.6158.
41. **Paprotka T, Deuschle K, Metzler V, Jeske H.** 2011. Conformation-selective methylation of geminiviral DNA. J Virol **85:**12001–12012. http://dx.doi.org/10.1128/JVI.05567-11.
42. **Pilartz M, Jeske H.** 2003. Mapping of Abutilon mosaic geminivirus minichromosomes. J Virol **77:**10808–10818. http://dx.doi.org/10.1128/JVI.77.20.10808-10818.2003.
43. **Frischmuth S, Frischmuth T, Jeske H.** 1991. Transcript mapping of Abutilon mosaic virus, a geminivirus. Virology **185:**596–604. http://dx.doi.org/10.1016/0042-6822(91)90530-O.
44. **Abouzid AM, Frischmuth T, Jeske H.** 1988. A putative replicative form of the Abutilon mosaic virus (gemini group) in a chromatin-like structure. Mol Gen Genet **212:**252–258. http://dx.doi.org/10.1007/BF00334693.
45. **Raja P, Jackel JN, Li S, Heard IM, Bisaro DM.** 2014. Arabidopsis double-stranded RNA binding protein DRB3 participates in methylation-mediated defense against geminiviruses. J Virol **88:**2611–2622. http://dx.doi.org/10.1128/JVI.02305-13.
46. **Paprotka T, Deuschle K, Pilartz M, Jeske H.** 2015. Form follows function in geminiviral minichromosome architecture. Virus Res **196:**44–55. http://dx.doi.org/10.1016/j.virusres.2014.11.004.
47. **Frischmuth T, Zimmat G, Jeske H.** 1990. The nucleotide sequence of abutilon mosaic virus reveals prokaryotic as well as eukaryotic features. Virology **178:**461–468. http://dx.doi.org/10.1016/0042-6822(90)90343-P.
48. **Silhavy D, Molnar A, Lucioli A, Szittya G, Hornyik C, Tavazza M, Burgyan J.** 2002. A viral protein suppresses RNA silencing and binds silencing-generated, 21- to 25-nucleotide double-stranded RNAs. EMBO J **21:**3070–3080. http://dx.doi.org/10.1093/emboj/cdf312.
49. **Koncz C, Martini N, Szabados L, Hrouda M, Bachmair A, Schell J.** 1994. Specialized vectors for gene tagging and expression studies, p 1–22. *In* Gelvin SB, Schilperoort RA (ed), Plant molecular biology manual, vol B2. Kluwer Academic Publishers, Dordrecht, Netherlands.
50. **Wege C, Jeske H.** 1998. Abutilon mosaic geminivirus proteins expressed and phosphorylated in Escherichia coli. J Phytopathol **146:**613–621. http://dx.doi.org/10.1111/j.1439-0434.1998.tb04763.x.
51. **Sambrook J, Russell DW.** 2001. Molecular cloning: a laboratory manual, 3rd ed. Cold Spring Harbor Laboratory Press, Cold Spring Harbor, NY.
52. **Ferrando A, Farras R, Jasik J, Schell J, Koncz C.** 2000. Intron-tagged epitope: a tool for facile detection and purification of proteins expressed in Agrobacterium-transformed plant cells. Plant J **22:**553–560. http://dx.doi.org/10.1046/j.1365-313x.2000.00763.x.
53. **Krenz B, Neugart F, Kleinow T, Jeske H.** 2011. Self-interaction of Abutilon mosaic virus replication initiator protein (Rep) in plant cell nuclei. Virus Res **161:**194–197. http://dx.doi.org/10.1016/j.virusres.2011.07.020.
54. **Wege C, Pohl D.** 2007. Abutilon mosaic virus DNA B component supports mechanical virus transmission, but does not counteract begomoviral phloem limitation in transgenic plants. Virology **365:**173–186. http://dx.doi.org/10.1016/j.virol.2007.03.041.
55. **Haseloff J, Siemering KR, Prasher DC, Hodge S.** 1997. Removal of a cryptic intron and subcellular localization of green fluorescent protein are required to mark transgenic Arabidopsis plants brightly. Proc Natl Acad Sci U S A **94:**2122–2127. http://dx.doi.org/10.1073/pnas.94.6.2122.
56. **Krenz B, Wege C, Jeske H.** 2010. Cell-free construction of disarmed Abutilon mosaic virus-based gene silencing vectors. J Virol Methods **169:**129–137. http://dx.doi.org/10.1016/j.jviromet.2010.07.010.
57. **van Engelen FA, Molthoff JW, Conner AJ, Nap JP, Pereira A, Stiekema W.** 1995. pBINPLUS: an improved plant transformation vector based on pBIN19. Transgenic Res **4:**288–290. http://dx.doi.org/10.1007/BF01969123.
58. **Morilla G, Castillo AG, Preiss W, Jeske H, Bejarano ER.** 2006. A versatile transreplication-based system to identify cellular proteins involved in geminivirus replication. J Virol **80:**3624–3633. http://dx.doi.org/10.1128/JVI.80.7.3624-3633.2006.
59. **Haible D, Kober S, Jeske H.** 2006. Rolling circle amplification revolutionizes diagnosis and genomics of geminiviruses. J Virol Methods **135:**9–16. http://dx.doi.org/10.1016/j.jviromet.2006.01.017.
60. **Papaefthimiou I, Hamilton AJ, Dentil MA, Baulcombe DC, Tsagris M, Tabler M.** 2001. Replicating potato spindle tuber viroid RNA is accompanied by short RNA fragments that are characteristic of post-transcriptional gene silencing. Nucleic Acids Res **29:**2395–2400. http://dx.doi.org/10.1093/nar/29.11.2395.
61. **Laemmli UK.** 1970. Cleavage of structural proteins during the assembly of the head of bacteriophage T4. Nature **227:**680–685. http://dx.doi.org/10.1038/227680a0.
62. **O'Farrell PZ, Goodman HM, O'Farrell PH.** 1977. High resolution two-dimensional electrophoresis of basic as well as acidic proteins. Cell **12:**1133–1142. http://dx.doi.org/10.1016/0092-8674(77)90176-3.
63. **Blum HE, Beier H, Gross HJ.** 1987. Improved silver staining of plant proteins, RNA and DNA in polyacrylamide gels. Electrophoresis **8:**93–99. http://dx.doi.org/10.1002/elps.1150080203.
64. **Thömmes PA, Buck KW.** 1994. Synthesis of the tomato golden mosaic virus AL1, AL2, AL3 and AL4 proteins in vitro. J Gen Virol **75:**1827–1834. http://dx.doi.org/10.1099/0022-1317-75-8-1827.
65. **Sung YK, Coutts RHA.** 1996. Potato yellow mosaic geminivirus AC2 protein is a sequence non-specific DNA binding protein. FEBS Lett **383:**51–54. http://dx.doi.org/10.1016/0014-5793(96)00217-7.
66. **Hipp K, Rau R, Schäfer B, Gronenborn B, Jeske H.** 2014. The RXL motif of the African cassava mosaic virus Rep protein is necessary for rereplication of yeast DNA and viral infection in plants. Virology **462–463:**189–198. http://dx.doi.org/10.1016/j.virol.2014.06.002.
67. **Kittelmann K, Rau P, Gronenborn B, Jeske H.** 2009. Plant geminivirus rep protein induces rereplication in fission yeast. J Virol **83:**6769–6778. http://dx.doi.org/10.1128/JVI.02491-08.
68. **Nagar S, Hanley-Bowdoin L, Robertson D.** 2002. Host DNA replication is induced by geminivirus infection of differentiated plant cells. Plant Cell **14:**2995–3007. http://dx.doi.org/10.1105/tpc.005777.
69. **Richter K, Kleinow T, Jeske H.** 2014. Somatic homologous recombination in plants is promoted by a geminivirus in a tissue-selective manner. Virology **452:**287–296. http://dx.doi.org/10.1016/j.virol.2014.01.024.
70. **Eagle PA, Hanley-Bowdoin L.** 1997. cis elements that contribute to geminivirus transcriptional regulation and the efficiency of DNA replication. J Virol **71:**6947–6955.
71. **Eagle PA, Orozco BM, Hanley-Bowdoin L.** 1994. A DNA sequence

required for geminivirus replication also mediates transcriptional regulation. Plant Cell **6:**1157–1170. http://dx.doi.org/10.1105/tpc.6.8.1157.
72. **Fontes EPB, Luckow VA, Hanley-Bowdoin L.** 1992. A geminivirus replication protein is a sequence-specific DNA binding protein. Plant Cell **4:**597–608. http://dx.doi.org/10.1105/tpc.4.5.597.
73. **Amrao L, Amin I, Shahid MS, Briddon RW, Mansoor S.** 2010. Cotton leaf curl disease in resistant cotton is associated with a single begomovirus that lacks an intact transcriptional activator protein. Virus Res **152:**153–163. http://dx.doi.org/10.1016/j.virusres.2010.06.019.
74. **Gopal P, Pravin Kumar P, Sinilal B, Jose J, Kasin Yadunandam A, Usha R.** 2007. Differential roles of C4 and betaC1 in mediating suppression of post-transcriptional gene silencing: evidence for transactivation by the C2 of Bhendi yellow vein mosaic virus, a monopartite begomovirus. Virus Res **123:**9–18. http://dx.doi.org/10.1016/j.virusres.2006.07.014.
75. **Dry I, Krake L, Mullineaux P, Rezaian A.** 2000. Regulation of tomato leaf curl viral gene expression in host tissues. Mol Plant Microbe Interact **13:**529–537. http://dx.doi.org/10.1094/MPMI.2000.13.5.529.
76. **Kleinow T, Bhalerao R, Breuer F, Umeda M, Salchert K, Koncz C.** 2000. Functional identification of an *Arabidopsis* Snf4 ortholog by screening for heterologous multicopy suppressors of *snf4* deficiency in yeast. Plant J **23:**115–122. http://dx.doi.org/10.1046/j.1365-313x.2000.00809.x.
77. **Kleinow T, Himbert S, Krenz B, Jeske H, Koncz C.** 2009. NAC domain transcription factor ATAF1 interacts with SNF1-related kinases and silencing of its subfamily causes severe developmental defects in Arabidopsis. Plant Sci **177:**360–370. http://dx.doi.org/10.1016/j.plantsci.2009.06.011.
78. **Kleinow T, Nischang M, Beck A, Kratzer U, Tanwir F, Preiss W, Kepp G, Jeske H.** 2009. Three C-terminal phosphorylation sites in the Abutilon mosaic virus movement protein affect symptom development and viral DNA accumulation. Virology **390:**89–101. http://dx.doi.org/10.1016/j.virol.2009.04.018.
79. **Kleinow T, Tanwir F, Kocher C, Krenz B, Wege C, Jeske H.** 2009. Expression dynamics and ultrastructural localization of epitope-tagged Abutilon mosaic virus nuclear shuttle and movement proteins in Nicotiana benthamiana cells. Virology **391:**212–220. http://dx.doi.org/10.1016/j.virol.2009.06.042.
80. **Krenz B, Windeisen V, Wege C, Jeske H, Kleinow T.** 2010. A plastid-targeted heat shock cognate 70 kDa protein interacts with the Abutilon mosaic virus movement protein. Virology **401:**6–17. http://dx.doi.org/10.1016/j.virol.2010.02.011.
81. **Dadami E, Dalakouras A, Zwiebel M, Krczal G, Wassenegger M.** 2014. An endogene-resembling transgene is resistant to DNA methylation and systemic silencing. RNA Biol **11:**934–941. http://dx.doi.org/10.4161/rna.29623.
82. **Krenz B, Jeske H, Kleinow T.** 2012. The induction of stromule formation by a plant DNA-virus in epidermal leaf tissues suggests a novel intra- and intercellular macromolecular trafficking route. Front Plant Sci **3:**291. http://dx.doi.org/10.3389/fpls.2012.00291.
83. **Pedersen TJ, Hanley-Bowdoin L.** 1994. Molecular characterization of the AL3 protein encoded by a bipartite geminivirus. Virology **202:**1070–1075. http://dx.doi.org/10.1006/viro.1994.1442.
84. **Haley A, Zhan X, Richardson K, Head K, Morris B.** 1992. Regulation of the activities of African cassava mosaic virus promoters by the AC1, AC2, and AC3 gene products. Virology **188:**905–909. http://dx.doi.org/10.1016/0042-6822(92)90551-Y.
85. **Settlage SB, See RG, Hanley-Bowdoin L.** 2005. Geminivirus C3 protein: replication enhancement and protein interactions. J Virol **79:**9885–9895. http://dx.doi.org/10.1128/JVI.79.15.9885-9895.2005.
86. **Orozco BM, Kong LJ, Batts LA, Elledge S, Hanley-Bowdoin L.** 2000. The multifunctional character of a geminivirus replication protein is reflected by its complex oligomerization properties. J Biol Chem **275:**6114–6122. http://dx.doi.org/10.1074/jbc.275.9.6114.
87. **Lozano-Duran R, Caracuel Z, Bejarano ER.** 2012. C2 from beet curly top virus meddles with the cell cycle: a novel function for an old pathogenicity factor. Plant Signal Behav **7:**1705–1708. http://dx.doi.org/10.4161/psb.22100.